$f(R,T)$ Cosmological Models in Phase Space

Hamid Shabani[1,*] and Mehrdad Farhoudi[1,†]

[1] *Department of Physics, Shahid Beheshti University, G.C., Evin, Tehran, 19839, Iran*

(Dated: August 18, 2013)

We investigate the cosmological solutions of $f(R,T)$ modified theories of gravity for a perfect fluid in a spatially FLRW metric through the phase space analysis, where R is the Ricci scalar and T denotes the trace of the energy–momentum tensor of the matter content. We explore and analyze the three general theories with the Lagrangians of minimal $g(R)+h(T)$, pure non–minimal $g(R)h(T)$ and non–minimal $g(R)\,(1+h(T))$ couplings through the dynamical systems approach. We introduce a few variables and dimensionless parameters to simplify the equations in more concise forms. The conservation of the energy–momentum tensor leads to a constraint equation that, in the minimal gravity, confines the functionality of $h(T)$ to a particular form, hence, relates the dynamical variables. In this case, the acceptable cosmological solutions that contain a long enough matter dominated era followed by a late–time accelerated expansion are found. To support the theoretical results, we also obtain the numerical solutions for a few functions of $g(R)$, and the results of the corresponding models confirm the predictions. We classify the solutions into six classes which demonstrate more acceptable solutions and there is more freedom to have the matter dominated era than in the $f(R)$ gravity. In particular, there is a new fixed point which can represent the late–time acceleration. We draw different diagrams of the matter densities (consistent with the present values), the related scale factors and the effective equation of state. The corresponding diagrams of the parameters illustrate that there is a saddle acceleration era which is a middle era before the final stable acceleration de Sitter era for some models. All presented diagrams determine radiation, matter and late–time acceleration eras very well. The pure non–minimal theory suffers from the absence of a standard matter era, though we illustrate that the non–minimal theory can have acceptable cosmological solutions.

PACS numbers: 04.50.Kd; 95.36.+x; 98.80.-k; 98.80.Jk
Keywords: Cosmology; $f(R,T)$ Gravity; Dark Energy; Dynamical Systems Approach; Modified Theories of Gravity.

I. INTRODUCTION

Since the birth of general relativity (GR) in 1915, the theory has faced the appearance of new ideas on changing or even replacing it in favor of an alternative one[1] which could solve different aspects or at least some parts of its incompleteness and shortcomings. These novel ideas mainly consist of some modifications or generalizations which would challenge GR in a geometrical background. Some of these theories introduce extra dimensions e.g., the Kaluza–Klein theories [3] and braneworld scenarios [4]. Other alternatives are scalar–tensor theories e.g., the Brans–Dicke theory [5] and higher–order/modified gravities [2, 6–12]. Another possibility is to introduce some new cosmic fluids e.g., dark matter [13–17], which should give rise to the clustered structures, and dark energy [18–22], which is responsible for the observed accelerated expansion of the universe. In particular, the following issues can be addressed as GR insufficiencies. Fundamentally, incompatibility with the quantum theory and observationally, inability to explain the flatness of galaxy rotation curves [23, 24]. Also, the existing problems of the isotropic and homogeneous cosmological solution of GR (the standard big–bang cosmology) such as the horizon and the flatness problems [25], and the absence of solution(s) including the well–accepted states of cosmological evolution in the past and future. That is, an accelerating phase solution prior to the radiation–dominated era e.g., inflation [26–30], and an acceleration phase needed to explain the present accelerated expansion observed by, e.g., the supernova Ia observations [31–35], the large–scale structure (LSS) [36, 37], the baryon acoustic oscillations (BAO) [38–40], the cosmic microwave background radiation (CMBR) [41–43] and the weak lensing [44]. Of course, in spite of the above deficiencies, matching the experimental results for the precession of the Mercury orbit [45–47], the Lense–Thirring gravitomagnetic precession [48], the gravitational deflection of light by the sun [45–47] and the gravitational redshift[2] [45–47] are the excellent successes of GR. On the whole, the results of Einsteins theory when considering the

* h_shabani@sbu.ac.ir
† m-farhoudi@sbu.ac.ir

[1] For example, see Refs. [1, 2] and references therein.

[2] However, any relativistic theory of gravitation consistent with the principle of equivalence will predict a redshift.

development of a general phenomenological framework, i.e. the PPN–formalism, determine that it is the best known metric theory of gravity [46].

Among the extended theories of gravity, there are at least two main motivations[3] for employing the higher–order gravities, i.e., those in which the Einstein–Hilbert action is modified by higher–order curvature invariants with respect to the Ricci scalar. The first motivation has a theoretical background and is related to the non–renormalizability of GR [49, 50] and to the fact that GR cannot be quantized conventionally. Regarding this issue, some authors have shown that the inclusion of higher–order terms can solve this problem [51, 52]. The other motivation is related to the recently achieved data in astrophysics and cosmology. Two contemporary evidences, which are referred to as dark matter and dark energy, have challenged our knowledge about the universe and have accounted for the first signals of GR breakdown. It is also worth mentioning that the concordance or ΛCDM model [53], the simplest model which adequately fits the present observations, supported by an inflation scenario,[4] can eventuate an accelerating phase in the very early and the late universe. However, the ΛCDM model suffers from the well–known cosmological problem originating in pertaining the cosmological constant to the vacuum energy [54–56]. That is, the cosmological constant is tremendously small with respect to the vacuum energy that is defined in particle physics. With regard to this, a mechanism is needed to get such a small value to match the present observations, e.g., dynamical dark energy models contain such mechanisms [57, 58].

$f(R)$ gravities, as the simplest family of the higher–order gravities, are obtained by replacing the Ricci scalar with a function $f(R)$ in the Einstein–Hilbert action. Generally, every new gravity theory, when is introduced as an alternative to GR, would be tested in two realms. That is, the weak field tests, i.e. those that can elaborate whether the theory leads to the known solar system observations, and the cosmological tests which inspect the theory aiming to find at least a solution that matches the present accelerated expansion observations. $f(R)$ gravity theories are not excepted from these examinations. In these issues, a few authors have claimed that the solar system tests rule out most $f(R)$ models [59–61], though others do not agree with these results [8]. However, these issues do not seem to be settled completely; see, e.g., Refs. [9, 12]. Despite the results of local gravity tests, one can still look at these theories for cosmological solutions as an independent criterion [62]. In this sense, these theories can be considered as $f(R)$ dark energy models implying that they can play the role of dark energy without using a cosmological constant, i.e., they can encompass these problems in a self–consistent scheme. Nevertheless, in addition to $f(R)$ gravities, there are numerous alternative gravity theories that claim to cure the problems of dark energy and inflation, in which up to now, the most physical contents of these theories have been widely explored; see, e.g., Refs. [2, 22].

In this work, we purpose to study the cosmology of the so–called $f(R,T)$ gravity, first introduced in Ref. [63] and then, studied in Refs. [64–71]. The theory of $f(R,T)$ gravity generalizes $f(R)$ theories of gravity by incorporation of the trace of energy–momentum tensor in addition to the Ricci scalar. The justification for the dependence on T comes from inductions arising from some exotic fluid and/or quantum effects (conformal anomaly[5]). Actually, this induction point of view adopts or links with the known proposals such as geometrical curvature inducing matter, a geometrical description of physical forces, and a geometrical origin for the matter content of the universe.[6] In Ref. [63], the field equations of some particular models are presented, and specially, scalar field models $f(R,T^{\phi})$ are analyzed in detail with a brief consideration of their cosmological implications. Also, the equation of motion of the test particle and the Newtonian limit of this equation are further analyzed in Ref. [63]. Up to now, the issues which have been investigated along with this modified theory are the energy conditions [65], the thermodynamics [66–68], anisotropic cosmology [69], the cosmology in which the representation employs an auxiliary scalar field [64], the reconstruction of some cosmological models [70] and the scalar perturbations [71]. Also, a further generalization of this theory has been proposed recently in Refs. [73, 74]. Incidentally, in the literature, authors have worked on a theory of gravity titled "the $f(T)$ gravity" (see, e.g., Ref. [75] and references therein), where T in this theory is the torsion scalar arising from the torsion tensor in a similar way as the curvature scalar arises from the curvature tensor, and which is completely different from $f(R,T)$ gravity.

On the other hand, $f(R,T)$ gravity may be considered as a correction or generalization of $f(R)$ gravities as long as the cosmological considerations are concerned. In this regard, we employ $f(R,T)$ gravity in an extended version and almost similar to the terminology employed for the $f(R)$ gravity in Ref. [76]. Hence, in the forthcoming sections, we theoretically investigate the cosmological solutions of $f(R,T)$ models and compare the results with the corresponding $f(R)$ cosmological models of Ref. [76]. To support the theoretical results, we also obtain the numerical solutions. In Sec. II, we derive the equations of motion (EOM) for $f(R,T)$ gravity and show that in this case, the conservation of the energy–momentum tensor leads to a constraint equation that must be satisfied by any function of $f(R,T)$. For example, for a minimal coupling form $f(R,T) = g(R) + h(T)$, this constraint restricts the form of function $h(T)$.

[3] See, e.g., Ref. [6].
[4] Such a scenario is needed because the accelerated phase in the very early universe should end to connect to a radiation dominated phase; however, a cosmological constant cannot fulfill this requirement [25].
[5] See, e.g., Refs. [49, 72].
[6] See, e.g., Refs. [1, 72] and references therein.

Then, we introduce a number of variables to simplify the equations in more concise forms for the later applications. In Sec. III, we analyze the cosmological solution through the dynamical systems approach. In this section, we consider the minimal combination, and obtain the corresponding solutions and the conditions for the existence of acceptable solutions. In Sec. IV, we investigate the numerical results for several functions of $f(R,T)$ in order to support the theoretical outcomes. In Secs. V and VI, we extend the discussion to the non–minimal combinations and finally, we summarize the obtained results in the last section.

II. FIELD EQUATIONS OF THE THEORY

In this section, we obtain the field equations of $f(R,T)$ gravity and then, introduce some dimensionless variables to simplify the corresponding equations. The action can be written in the form

$$S=\int\sqrt{-g}d^4x\left[\frac{1}{16\pi G}f(R,T^{(\mathrm{m})})+L^{(\mathrm{m})}+L^{(\mathrm{rad})}\right], \tag{2.1}$$

where R is the Ricci scalar, $T^{(\mathrm{m})}\equiv g^{\mu\nu}T^{(\mathrm{m})}_{\mu\nu}$ is the trace of the energy–momentum tensor, the superscript m stands for the dust matter, $f(R,T^{(\mathrm{m})})$ is an arbitrary function of the Ricci scalar and $T^{(\mathrm{m})}$, $L^{(\mathrm{m})}$ and $L^{(\mathrm{rad})}$ are the Lagrangians of the dust matter and radiation, g is the determinant of the metric and we set $c=1$. As $T^{(\mathrm{rad})}=0$, the trace of the radiation energy–momentum tensor does not play any role in the function of $f(R,T^{(\mathrm{m})})$ and henceforth, from now on we drop the superscript m from the trace $T^{(\mathrm{m})}$ unless it is necessary. The energy–momentum tensor is usually defined as the Euler–Lagrange expression of the matter Lagrangian, i.e.,

$$T_{\mu\nu}\equiv-\frac{2}{\sqrt{-g}}\frac{\delta\left[\sqrt{-g}(L^{(\mathrm{m})}+L^{(\mathrm{rad})})\right]}{\delta g^{\mu\nu}}, \tag{2.2}$$

and if one assumes that both the Lagrangians depend only on the metric and not on its derivatives, one will get

$$T_{\mu\nu}=g_{\mu\nu}[L^{(\mathrm{m})}+L^{(\mathrm{rad})}]-2\frac{\partial[L^{(\mathrm{m})}+L^{(\mathrm{rad})}]}{\partial g^{\mu\nu}}. \tag{2.3}$$

By the metric variation of action (2.1), the field equations are[7]

$$F(R,T)R_{\mu\nu}-\frac{1}{2}f(R,T)g_{\mu\nu}+\Big(g_{\mu\nu}\Box-\nabla_\mu\nabla_\nu\Big)F(R,T)=\Big(8\pi G+\mathcal{F}(R,T)\Big)T^{(\mathrm{m})}_{\mu\nu}+8\pi GT^{(\mathrm{rad})}_{\mu\nu}, \tag{2.4}$$

where it is helpful to define the derivatives with respect to the trace T and the Ricci scalar R as

$$\mathcal{F}(R,T)\equiv\frac{\partial f(R,T)}{\partial T}\qquad\text{and}\qquad F(R,T)\equiv\frac{\partial f(R,T)}{\partial R}, \tag{2.5}$$

and we have used

$$g^{\alpha\beta}\frac{\delta T^{(\mathrm{m})}_{\alpha\beta}}{\delta g^{\mu\nu}}=-2T^{(\mathrm{m})}_{\mu\nu}. \tag{2.6}$$

Also, by contracting equation (2.4), we have

$$F(R,T)R+3\Box F(R,T)-2f(R,T)=\Big(8\pi G+\mathcal{F}(R,T)\Big)T. \tag{2.7}$$

Now, in this model, we assume a perfect fluid and a spatially flat Friedmann–Lemaître–Robertson–Walker (FLRW) metric

$$ds^2=-dt^2+a^2(t)\Big(dx^2+dy^2+dz^2\Big), \tag{2.8}$$

---

[7] By the variational (functional) derivative procedure (see, e.g., Refs. [1, 77]) and employing the Palatini equation (identity), one can usually derive field equations; nevertheless, one can consult the detailed derivation of these field equations in Ref. [63].

where $a(t)$ is the scale factor. Let us rewrite equation (2.4) in a standard form similar to GR, i.e.,

$$G_{\mu\nu} = \frac{8\pi G}{F(R,T)}\left(T^{(\mathrm{m})}_{\mu\nu} + T^{(\mathrm{rad})}_{\mu\nu} + T^{(\mathrm{eff})}_{\mu\nu}\right), \tag{2.9}$$

where

$$T^{(\mathrm{eff})}_{\mu\nu} \equiv \frac{1}{8\pi G}\left[\frac{1}{2}\Big(f(R,T) - F(R,T)R\Big)g_{\mu\nu} + \Big(\nabla_\mu\nabla_\nu - g_{\mu\nu}\Box\Big)F(R,T) + \mathcal{F}(R,T)T^{(\mathrm{m})}_{\mu\nu}\right]. \tag{2.10}$$

Regarding the Bianchi identity,[8] obviously in $f(R,T)$ gravity, the above effective energy–momentum tensor is not conserved. Thus, by applying the conservation of the energy–momentum tensor of all matter and knowing that $\nabla^\mu T^{(\mathrm{m})}_{\mu\nu} = 0 = \nabla^\mu T^{(\mathrm{rad})}_{\mu\nu}$, the following constraint must hold. That is

$$\frac{3}{2}H(t)\mathcal{F}(R,T) = \dot{\mathcal{F}}(R,T), \tag{2.11}$$

where dot denotes the derivative with respect to the cosmic time t and $H(t) = \dot{a}(t)/a(t)$ is the Hubble parameter. Obviously this relation leads to some restrictions on the functionality of $f(R,T)$, as we shall see in the next section. Equations (2.4) and (2.7), by assuming metric (2.8), give

$$3H^2F(R,T) + \frac{1}{2}\Big(f(R,T) - F(R,T)R\Big) + 3\dot{F}(R,T)H = \Big(8\pi G + \mathcal{F}(R,T)\Big)\rho^{(\mathrm{m})} + 8\pi G\rho^{(\mathrm{rad})} \tag{2.12}$$

as the Friedmann–like equation, and

$$2F(R,T)\dot{H} + \ddot{F}(R,T) - \dot{F}(R,T)H = -\Big(8\pi G + \mathcal{F}(R,T)\Big)\rho^{(\mathrm{m})} - \frac{32}{3}\pi G\rho^{(\mathrm{rad})} \tag{2.13}$$

as the Raychaudhuri–like equation.

In the following, we assume those functions of $f(R,T)$ that can be explicitly written as combinations of a function $g(R)$ and a function $h(T)$, e.g., $f(R,T) = g(R)h(T)$; however, due to the constraint equation (2.11), their forms would be restricted. Now, it is convenient to introduce a few dimensionless independent variables to simplify the obtained equations in the phase space, used in the following sections. These variables are defined as

$$x_1 \equiv -\frac{\dot{g}'(R)}{Hg'(R)}, \tag{2.14}$$

$$x_2 \equiv -\frac{g(R)}{6H^2g'(R)}, \tag{2.15}$$

$$x_3 \equiv \frac{R}{6H^2} = \frac{\dot{H}}{H^2} + 2, \tag{2.16}$$

$$x_4 \equiv -\frac{h(T)}{3H^2g'(R)}, \tag{2.17}$$

$$x_5 \equiv \frac{8\pi G\rho^{(\mathrm{rad})}}{3H^2g'(R)}, \tag{2.18}$$

$$x_6 \equiv -\frac{Th'(T)}{3H^2g'(R)}, \tag{2.19}$$

where the prime denotes the ordinary derivative with respect to the argument and we have used $R = 6(\dot{H} + 2H^2)$ for metric (2.8). However, it will be shown in Sec. III that these six variables of the phase space reduce to five independent variables once the constraint equation (2.11) is applied. One may also define some other dimensionless parameters

[8] It is well–known that the use of the action principle and the principle of general invariance allows immediate connections between symmetry principles and conservation laws to be established as inner identities. That is, the metric variation of each Lagrangian density (as a scalar density) of weight one, which is a function of the metric and its derivatives, makes the covariant divergence of the Euler–Lagrange expression of the Lagrangian density identically vanish, e.g., $\nabla^\mu T_{\mu\nu} \equiv 0$; see any text on gravitation, e.g., Ref. [78].

that can play the role of parametrization in the determination of the function $f(R,T)$, namely,

$$m \equiv \frac{Rg''(R)}{g'(R)}, \tag{2.20}$$

$$r \equiv -\frac{Rg'(R)}{g(R)} = \frac{x_3}{x_2}, \tag{2.21}$$

$$n \equiv \frac{Th''(T)}{h'(T)}, \tag{2.22}$$

$$s \equiv \frac{Th'(T)}{h(T)} = \frac{x_6}{x_4}, \tag{2.23}$$

where $g(R) \neq$ constant and $h(T) \neq$ constant. Note that, generally, we have[9] $m = m(r)$ and $n = n(s)$.

One knows that from the Friedmann equations in GR with the FLRW metric, the relation $w = p/\rho = -1-2\dot{H}/3H^2$ for the equation of state is obtained. Analogously, if one correspondingly defines an effective equation of state (for an effective pressure and an effective energy density) as $w^{(\mathrm{eff})} = p^{(\mathrm{eff})}/\rho^{(\mathrm{eff})} \equiv -1 - 2\dot{H}/3H^2$ then, one will obtain the effective equation of state as follows. At first, let us redefine equations (2.12) and (2.13) in a more useful manner for matching with the SN Ia observations, as

$$3AH^2 = 8\pi G(\rho^{(\mathrm{m})} + \rho^{(\mathrm{rad})} + \rho^{(\mathrm{DE})}) \tag{2.24}$$

and

$$-2A\dot{H} = 8\pi G\Big(\rho^{(\mathrm{m})} + (4/3)\rho^{(\mathrm{rad})} + \rho^{(\mathrm{DE})} + p^{(\mathrm{DE})}\Big), \tag{2.25}$$

where A is a constant and $\rho^{(\mathrm{DE})}$ and $p^{(\mathrm{DE})}$ denote the density and the pressure of the dark energy, defined as

$$8\pi G\rho^{(\mathrm{DE})} \equiv \mathcal{F}\rho^{(\mathrm{m})} - 3\dot{F}(R,T)H - \frac{1}{2}\Big(f(R,T) - F(R,T)R\Big) + 3H^2(A - F) \tag{2.26}$$

and

$$8\pi G p^{(\mathrm{DE})} \equiv \ddot{F}(R,T) + 2\dot{F}(R,T)H + \frac{1}{2}\Big(f(R,T) - F(R,T)R\Big) - (2\dot{H} + 3H^2)(A - F). \tag{2.27}$$

Thus, the equation of state parameter for the dark energy is given as $w^{(\mathrm{DE})} \equiv p^{(\mathrm{DE})}/\rho^{(\mathrm{DE})}$.

Definitions (2.26) and (2.27) lead to the continuity equation for the dark energy component, namely,

$$\dot{\rho}^{(\mathrm{DE})} + 3H(\rho^{(\mathrm{DE})} + p^{(\mathrm{DE})}) = 0. \tag{2.28}$$

Now, we can rewrite the effective equation of state in the following form

$$w^{(\mathrm{eff})} = \frac{F}{A}\Big(\Omega^{(\mathrm{DE})}w^{(\mathrm{DE})} + \frac{\Omega^{(\mathrm{rad})}}{3}\Big), \tag{2.29}$$

where we have defined

$$\Omega^{(\mathrm{rad})} \equiv \frac{8\pi G\rho^{(\mathrm{rad})}}{3H^2F} \qquad \text{and} \qquad \Omega^{(\mathrm{DE})} \equiv \frac{8\pi G\rho^{(\mathrm{DE})}}{3H^2F}, \tag{2.30}$$

which lead to the usual density parameters for GR. Using definition (2.16), w^{eff} reads in a suitable form

$$w^{(\mathrm{eff})} = \frac{1}{3}(1 - 2x_3). \tag{2.31}$$

Also, for a general matter, the cosmological solutions, for a constant value of x_3, can be found from equations (2.16) to be

$$a(t) = a_0\left(\frac{t - t_i}{t_0 - t_i}\right)^{\frac{1}{2-x_3}} \tag{2.32}$$

---

[9] Actually, in principle, one can derive R and T from definitions (2.21) and (2.23) in terms of r and s, respectively. Hence, one gets $m = m(r)$ and $n = n(s)$.

and, for the conservation of the energy–momentum tensor one has

$$\dot{\rho}(t) + 2\,(2 - x_3)\,H(t)\rho(t) = 0, \tag{2.33}$$

where a_0 and t_0 are the integral constants that can be fixed by the present values, and for t_i, we set $a(t_i) = 0$. Equations (2.32) and (2.33) hold for all values of x_3 except for $x_3 = 2$. In this special case we have $\dot{H} = 0$, which leads to either a de Sitter solution or a static one.

In the next section, we consider a particular form of the function $f(R,T)$ and show that the acceptable solution trajectories tend to transit from the radiation era with $x_3 = 0$ to the dust–like matter era with $x_3 = 1/2$, where, for these two values, the conservation equation (2.33) gives,[10] respectively,

$$\dot{\rho}^{(\mathrm{rad})} + 4H\rho^{(\mathrm{rad})} = 0 \tag{2.34}$$

and

$$\dot{\rho}^{(m)} + 3H\rho^{(m)} = 0. \tag{2.35}$$

III. DYNAMICAL SYSTEMS APPROACH OF THE MINIMAL CASE $f(R,T) = g(R) + h(T)$

In this section, we investigate the model, by employing the dynamical systems approach, first when the geometrical sector and the matter sector in the function $f(R,T)$ are minimally coupled.[11] The cases of non–minimal coupling are considered in the later sections. In the minimal case, we assume that the form of function $f(R,T)$ is

$$f(R,T) = g(R) + h(T), \tag{3.1}$$

where $h(T)$ and $g(R)$ are arbitrary functions and hereafter, we show the functions $g(R)$, $h(T)$ and their derivatives without indicating their arguments for the sake of convenience.

The dynamical systems approach[12] introduces a relatively simple technique to investigate whole space of solutions in the form of some extremum points (the fixed points), by which the evolution of system can be pictured qualitatively near these points. A qualitative study is possible via checking the phase space trajectories, whose behaviors are sensitive to initial conditions. In this way, one can obtain different descriptions dependent on different initial conditions and therefore, indicates those initial conditions that lead to a desired physical result. In cosmological applications, by this technique, one is capable of determining the early and the late time behaviors of models (in addition to possible matter or radiation solutions). That is, one can achieve a global picture of all solutions and behaviors of the system near these solutions. As a result, through the dynamical systems approach, the inconsistent models can be ruled out, and also those models which deserve further investigation could be selected. For a recent application of the dynamical systems approach to some modified theories of gravity see, e.g., Refs. [80–82].

Now, rewriting equations (2.12) and (2.13) with (3.1) gives

$$1 + \frac{g}{6H^2g'} + \frac{h}{6H^2g'} - \frac{R}{6H^2} + \frac{\dot{g'}}{Hg'} = \frac{8\pi G\rho^{(\mathrm{m})}}{3H^2g'} + \frac{h'\rho^{(\mathrm{m})}}{3H^2g'} + \frac{8\pi G\rho^{(\mathrm{rad})}}{3H^2g'} \tag{3.2}$$

and

$$2\frac{\dot{H}}{H^2} + \frac{\ddot{g'}}{H^2g'} - \frac{\dot{g'}}{Hg'} = -\frac{8\pi G\rho^{(\mathrm{m})}}{H^2g'} - \frac{h'\rho^{(\mathrm{m})}}{H^2g'} - \frac{32\pi G\rho^{(\mathrm{rad})}}{3H^2g'}. \tag{3.3}$$

In the approach of dynamical systems, original EOM (e.g., equations (3.2) and (3.3) in this work) can be cast in the form of some new evolutionary EOM in terms of new variables (which are constructed from the original ones) and their first derivatives. Then, the solutions of these new EOM are indicated as some fixed points of the system which are obtained through an extremization, where if the new EOM do not explicitly contain time then, the system will be called an autonomous one. We employ this approach to extract and analyze the solutions of equations (3.2) and (3.3) by employing the introduced variables (2.14)–(2.23).

---

[10] The radiation and the dust–like types of matters, analogously, are dictated from the appearance of the corresponding equations.

[11] We apply the conventional terminology used in the literature for adding and crossing two terms in the Lagrangian as the minimal and the non–minimal couplings, respectively.

[12] See Ref. [79] and references therein.

First of all, constraint (2.11), for the minimal case with $h \neq$ constant, gives

$$Th'' = -\frac{1}{2}h', \tag{3.4}$$

i.e., by (2.22), $n = -1/2$, and by integrating with respect to the trace T, reads

$$Th' - \frac{1}{2}h + C = 0, \tag{3.5}$$

where C is an integration constant. This constant must be zero to be consistent with condition (3.16), as we will show. Thus, equation (3.5) with $C = 0$ leads to $s = 1/2$ and hence, the relation $x_6 = x_4/2$. Therefore, with these unique constants n and s, the phase space variables of the model are reduced from six to five. As we will see, this reduction makes the problem to become more tractable than if there is not such a reduction.

Obviously, all cases with $x_4 = 0$ (for a non–singular denominator in (2.17)), in the minimal case, get returned to $f(R)$ gravity, however, the cases with non–zero x_4 give more general solutions than $f(R)$ gravity. Also, all cases with $h =$ constant can be considered in $f(R)$ gravity background and act as if they have a cosmological constant. Here, by applying equation (3.4), the only form that respects the conservation law, in the minimal case, is

$$f(R,T) = g(R) + c_1\sqrt{-T} + c_2, \tag{3.6}$$

where c_1 and c_2 are some constants with respect to T, however, they, in general, can be functions of the Ricci scalar R. Those cases in which c_1 is a function of R will be considered as a non–minimal case in the subsequent section. Now, let us obtain the possible "good" cosmological solutions, i.e. those solutions that describe a dust–like matter dominated era followed by an accelerated era, for the general case (3.6).

Equation (3.2) gives a constraint that must hold for the defined variables (2.14)–(2.18) as

$$\Omega^{(\mathrm{m})} \equiv \frac{8\pi G\rho^{(\mathrm{m})}}{3H^2 g'} = 1 - x_1 - x_2 - x_3 - x_4 - x_5. \tag{3.7}$$

Hence, the autonomous EOM for the five independent variables (2.14)–(2.18) can be achieved via

$$\frac{dx_1}{dN} = -1 + x_1(x_1 - x_3) - 3x_2 - x_3 - \frac{3}{2}x_4 + x_5, \tag{3.8}$$

$$\frac{dx_2}{dN} = \frac{x_1 x_3}{m} + x_2\left(4 + x_1 - 2x_3\right), \tag{3.9}$$

$$\frac{dx_3}{dN} = -\frac{x_1 x_3}{m} + 2x_3\left(2 - x_3\right), \tag{3.10}$$

$$\frac{dx_4}{dN} = x_4\left(\frac{5}{2} + x_1 - 2x_3\right), \tag{3.11}$$

$$\frac{dx_5}{dN} = x_5\left(x_1 - 2x_3\right), \tag{3.12}$$

where N represents derivative with respect to $\ln a$ and equation (3.7) has been used. The solutions for the system of equations (3.8)–(3.12) for arbitrary $m(r)$, $n(s) = -1/2$ and $s = 1/2$ are listed in Table 1. These solutions include ten fixed points P_1–P_{10} at which the variables x_1–x_5 (and any arbitrary function of them) take their critical values, i.e. these solutions are those of the system of equations $dx_i/dN = 0,\ i = 1, \cdots, 5$. Thus, in general, the parameters $r = r(x_2, x_3)$ and $s = s(x_4, x_6)$ must take their critical values too. That is,

$$\frac{dr}{dN} = \frac{\partial r(x_2,x_3)}{\partial x_2}\frac{dx_2}{dN} + \frac{\partial r(x_2,x_3)}{\partial x_3}\frac{dx_3}{dN} = 0 \tag{3.13}$$

and

$$\frac{ds}{dN} = \frac{\partial s(x_4,x_6)}{\partial x_4}\frac{dx_4}{dN} + \frac{\partial s(x_4,x_6)}{\partial x_6}\frac{dx_6}{dN} = 0, \tag{3.14}$$

which, using definitions (2.15)–(2.17) and (2.19)–(2.23), give

$$0 = \frac{dr}{dN} = -r\left(\frac{1 + r + m(r)}{m(r)}\right)x_1 \equiv -r\mathcal{M}(r)x_1 \tag{3.15}$$

and

$$0=\frac{ds}{dN}=3s\Big(s-n(s)-1\Big), \tag{3.16}$$

where we have defined

$$\mathcal{M}(r)\equiv\frac{1+r+m(r)}{m(r)}, \tag{3.17}$$

which is well–defined for $m(r)\neq 0$.[13] As a result, the condition $ds/dN=0$ for $s\neq 0$,[14] with $n=-1/2$, leads to $s=1/2$ which in turn gives the constant C in equation (3.5) to be zero. The acceptable solutions are those that respect these two conditions dr/dN=0 and $ds/dN=0$. Now, restoring constraint (2.11), from equations (3.15) and (3.16), it turns out that all acceptable solutions must lie in one of the following three categories

$$\begin{cases} 1)\ r=0,\ s=\frac{1}{2}=-n, \\ 2)\ \mathcal{M}(r)=0,\ s=\frac{1}{2}=-n, \\ 3)\ x_1=0,\ s=\frac{1}{2}=-n. \end{cases} \tag{3.18}$$

Table 1. The fixed points solutions of the dynamical systems approach of $f(R,T)=g(R)+h(T)$.

Fixed point	Coordinates (x_1,x_2,x_3,x_4,x_5)	Scale factor	$\Omega^{(\mathrm{m})}$	$\Omega^{(\mathrm{rad})}$	$w^{(\mathrm{eff})}$
P_1	$\left(\frac{3m}{2(1+m)},-\frac{5+8m}{4(1+m)^2},\frac{5+8m}{4(1+m)},\frac{4-m(3+10m)}{4(1+m)^2},0\right)$	$a(t)=a_0\left(\frac{t-t_i}{t_0-t_i}\right)^{\frac{4(1+m)}{3}}$	0	0	$-\frac{1+2m}{2(1+m)}$
P_2	$\left(\frac{2(1-m)}{1+2m},\frac{1-4m}{m(1+2m)},-\frac{(1-4m)(1+m)}{m(1+2m)},0,0\right)$	$a(t)=a_0\left(\frac{t-t_i}{t_0-t_i}\right)^{\frac{m(1+2m)}{1-m}}$	0	0	$\frac{2-5m-6m^2}{3m(1+2m)}$
P_3	$\left(\frac{3m}{1+m},-\frac{1+4m}{2(1+m)^2},\frac{1+4m}{2(1+m)},0,0\right)$	$a(t)=a_0\left(\frac{t-t_i}{t_0-t_i}\right)^{\frac{2(1+m)}{3}}$	$\frac{2-m(3+8m)}{2(1+m)^2}$	0	$-\frac{m}{1+m}$
P_4	$(-4,5,0,0,0)$	$a(t)=a_0\left(\frac{t-t_i}{t_0-t_i}\right)^{\frac{1}{2}}$	0	0	$\frac{1}{3}$
P_5	$\left(-\frac{5}{2},0,0,\ \frac{7}{2},0\right)$	$a(t)=a_0\left(\frac{t-t_i}{t_0-t_i}\right)^{\frac{1}{2}}$	0	0	$\frac{1}{3}$
P_6	$(-1,0,0,0,0)$	$a(t)=a_0\left(\frac{t-t_i}{t_0-t_i}\right)^{\frac{1}{2}}$	2	0	$\frac{1}{3}$
P_7	$(1,0,0,0,0)$	$a(t)=a_0\left(\frac{t-t_i}{t_0-t_i}\right)^{\frac{1}{2}}$	0	0	$\frac{1}{3}$
P_8[a]	$(0,-1,2,0,0)$	$a(t)=a_0\exp H_0t$	0	0	-1
P_9	$(0,0,0,0,1)$	$a(t)=a_0\left(\frac{t-t_i}{t_0-t_i}\right)^{\frac{1}{2}}$	0	1	$\frac{1}{3}$
P_{10}	$\left(\frac{4m}{1+4m},-\frac{2m}{(1+m)^2},\frac{2m}{1+m},0,\frac{1-m(2+5m)}{(1+m)^2}\right)$	$a(t)=a_0\left(\frac{t-t_i}{t_0-t_i}\right)^{\frac{1+m}{2}}$	0	$\frac{1-m(2+5m)}{(1+m)^2}$	$\frac{1-3m}{3(1+m)}$

[a] This solution has $\dot{H}=0$.

A glance at Table 1 shows that the points P_1, P_2, P_3 and P_{10} satisfy the condition $m(r)=-r-1$, the parameter r vanishes for the point P_4, and for the points P_8 and P_9, we have $x_1=0$. These are the only obvious points that respect (3.18). The other points have both $x_2=0$ and $x_3=0$, which implies that there is an ambiguity in determining r clearly. Nevertheless, these points actually do satisfy equations (3.15) and (3.16) and hence, r can be determined by a straightforward calculation using definition (2.21). In this respect, we consider that the condition $m(r)=-r-1$ should be valid for all of the points, and use it wherever it is necessary.

In the following discussions, the stability analysis of the fixed points are performed via inspecting the corresponding eigenvalues of them. Imprecisely speaking, the trajectories of the phase space advance to a fixed point if all eigenvalues have negative values, and recede from a fixed point if all eigenvalues have positive values. In this respect, the fixed points occurring in the former and the latter sets are called the stable and unstable points, respectively. The fixed points with both positive and negative eigenvalues are called saddle points, and those trajectories which advance to a saddle fixed point along some eigenvectors may recede from it along some other eigenvectors.

---

[13] Note that, all solutions that satisfy $m(r)=-r-1$ must satisfy $\mathcal{M}(r)=0$ as a more strong constraint, this fact affects the analysis involved in Sec. IV.

[14] Note that, the corresponding solutions with $s=0$ have been discarded, for they contradict with the former result $n=-1/2$.

In Subsection III A, we investigate the properties of each of the fixed points of Table 1 in the absence of the radiation. Since the calculations in a system with five degrees of freedom can be very messy and time consuming to study, we consider the effects of the radiation in Subsection III B. Also, in Subsection III C, we illustrate "good" cosmological solutions, i.e. those solutions that determine the trajectories which connect the dust–matter dominated points to the accelerated expansion dominated points. Incidentally, the considerations have been assisted by numerical manipulations wherever the exact computations have not been possible.

A. Properties of Fixed Points in the Absence of Radiation

In the absence of radiation, there are only the first eight fixed points P_1–P_8. While presenting the properties of these points, we compare the results with the corresponding results of the $f(R)$ gravity in Ref. [76] (whenever it is necessary), and briefly indicate the obtained results in Table 2.

- The Point P_1

  This is a new fixed point which corresponds to a curvature–dominated point![15] This point can play the role of an accelerated expansion point provided that $w^{(\rm eff)} < -1/3$ for $m > -1/4$ and $m < -1$. In the former range, we have a non–phantom accelerated universe, and the latter one lies in a phantom domain. The eigenvalues of this point are obtained as

$$-\frac{3}{2}, \qquad -\frac{3m(1+m)(3+2m)+a(m)}{8m(1+m)^2}, \qquad \frac{-3m(1+m)(3+2m)+a(m)}{8m(1+m)^2}, \qquad \frac{3}{2}(1+m'), \tag{3.19}$$

  where

$$a(m) \equiv \left\{ m(1+m)^2\Big[-160 + m(-55+700m+676m^2)\Big]\right\}^{1/2}, \tag{3.20}$$

  and $m' \equiv dm/dr$. The above eigenvalues show that with $m' > -1$, we have a saddle point. However, for $m' < -1$, the point P_1 is a stable point when $-4/5 < m < -5/8$ or $0.43 < m < 1/2$ with real valued eigenvalues, a spiral stable point when $0 < m \leq 0.43$ and a saddle point otherwise. Nevertheless, within these ranges, the first one does not lead to the condition $w^{(\rm eff)} < -1/3$ and hence, we discard it. As a result, the point P_1 introduces two new ranges that can accelerate universe in the non–phantom domain, which collectively are

$$m' < -1, \qquad 0 < m < \frac{1}{2}, \qquad -\frac{2}{3} < w^{(\rm eff)} < -\frac{1}{2}. \tag{3.21}$$

  In the limit $\mid m \mid \to 0$, the eigenvalues take the values

$$-\frac{3}{2}, \qquad -\frac{9}{8}+\sqrt{-\frac{5}{2m}}, \qquad -\frac{9}{8}-\sqrt{-\frac{5}{2m}}, \qquad \frac{3}{2}(1+m'). \tag{3.22}$$

  It means that, for $m \to 0^+$, this point is a spiral stable point when $m' < -1$ and a saddle one otherwise. When $\mid m \mid \to \infty$, the point tends to a de Sitter point with coordinates $(3/2,\ 0,\ 2,\ -5/2)$, which is not a stable point. Indeed, from (3.19), it is obvious that P_1 is a permanent saddle point in the both limits $m' = 0$ and $\mid m \mid \to \infty$.

- The Point P_2

  The point P_2 has also $\Omega^{(\rm m)} = 0 = \Omega^{(\rm rad)}$, and like P_1 is a curvature–dominated point whose effective equation of state depends on the parameter m. An accelerated expansion behavior can be achieved when $m < (-1-\sqrt{3})/2$ or $(-1+\sqrt{3})/2 < m < 1$ in the non–phantom domain, and when $-1/2 < m < 0$ or $m > 1$ in the phantom domain. The eigenvalues are obtained to be

$$-4+\frac{1}{m}, \qquad \frac{-8m^2-3m+2}{m(1+2m)}, \qquad \frac{2(1-m^2)(1+m')}{m(1+2m)}, \qquad \frac{-10m^2-3m+4}{2m(1+2m)}. \tag{3.23}$$

---

[15] We refer to a point with both properties $\Omega^{(\rm m)} = 0 = \Omega^{(\rm rad)}$ as a curvature–dominated point.

In the limit $\mid m \mid \to \infty$, it asymptotically reaches the point $P_{2,\rm dS} = (-1,\ 0,\ 2,\ 0)$, at which universe expands as a de Sitter accelerated one, and is a stable point for $m' > -1$. In the opposite limit, when $\mid m \mid \to 0$, the eigenvalues take the following forms

$$\frac{1}{m}, \quad \frac{2}{m}, \quad \frac{2}{m}(1+m'), \quad \frac{2}{m}.$$

Thus, in order to have a stable acceleration era, one must have $m \to 0^-$ and $m' > -1$, simultaneously. An investigation of the eigenvalues gives ranges of m, in which one can expect a stable accelerated expansion behavior. For the non–phantom domain, we have

$$\mathcal{A})\ \ m' > -1, \qquad m < -\frac{1}{2}(1+\sqrt{3}), \qquad -1 < w^{(\rm eff)} < -\frac{1}{3}, \tag{3.24}$$

$$\mathcal{B})\ \ m' < -1, \qquad \frac{1}{2} < m < 1, \qquad -1 < w^{(\rm eff)} < -\frac{2}{3}, \tag{3.25}$$

and for the phantom domain, we obtain

$$\mathcal{C})\ \ m' > -1, \qquad m > 1, \qquad -1.07 < w^{(\rm eff)} < -1, \tag{3.26}$$

$$\mathcal{D})\ \ m' > -1, \qquad -\frac{1}{2} < m < 0, \qquad w^{(\rm eff)} < -7.60. \tag{3.27}$$

However, P_2 is an unstable point in the range $0 < m < 1/4$ provided that $m' > -1$. The properties of this point do not change in this model compared to the $f(R)$ gravity, except in the case $\mathcal{B}$, where the range m becomes more restricted, i.e. the corresponding range is $(\sqrt{3}-1)/2 < m < 1$ in the case $\mathcal{B}$ in the $f(R)$ gravity.

- The Point P_3

The point through which we can search for a matter era is P_3, which also appears in the $f(R)$ gravity. For $m = 0$, we have $w^{(\rm eff)} = 0$ and $\Omega^{(\rm m)} = 1$. The eigenvalues are

$$\frac{3}{2}, \quad \frac{-3m + b(m)}{4m(1+m)}, \quad \frac{-3m - b(m)}{4m(1+m)}, \quad 3(1+m'), \tag{3.28}$$

where

$$b(m) \equiv \Big[m\big(256m^3 + 160m^2 - 31m - 16\big)\Big]^{1/2}. \tag{3.29}$$

The existence of the positive constant eigenvalue $3/2$ makes the point P_3 not to be a stable point, instead, it is always a saddle point. It is an interesting result that does not occur in the $f(R)$ gravity. For infinitesimal values of the parameter m, we can approximate the eigenvalues as

$$\frac{3}{2}, \quad -\frac{3}{4} + \sqrt{-\frac{1}{m}}, \quad -\frac{3}{4} - \sqrt{-\frac{1}{m}}, \quad 3(1+m'). \tag{3.30}$$

In the limit $m \to 0^+$, we have an acceptable saddle point matter era. However, the point P_3, in the limit $m \to 0^-$ is not generally acceptable, for the second eigenvalue becomes a large positive real value. Therefore, the matter era becomes very short, so that the observational data cannot be matched. The point P_3 contains some ranges in which universe can be accelerated, but not in a usual way, for, the accelerating conditions are

$$\mathcal{E})\ m > \frac{1}{2}, \qquad -1 < w^{(\rm eff)} < -\frac{1}{3}, \qquad -4 < \Omega^{(m)} < -\frac{1}{3}, \tag{3.31}$$

$$\mathcal{F})\ m < -1, \qquad w^{(\rm eff)} < -1, \qquad \Omega^{(m)} < -4. \tag{3.32}$$

That is, the accelerated expansion can occur with a negative value for the matter density parameter, which is not physically interesting. Considering the definition used in relation (3.7), the solutions denoting $\Omega^{(\rm m)} < 0$ are ruled out in the background of viable $f(R)$ models with the condition[16] $g'(R) > 0$, which we have also adopted here.

---

[16] This condition guaranties that the gravity force is an attractive one. As $f(R)$ theories are special cases with $h(T) = 0$ in the minimal coupling case, hence, this condition should hold.

- The Points P_4, P_5 and P_7

  There are three points in $f(R,T)$ gravity with $\Omega^{(\mathrm{m})}=0$ and $\Omega^{(\mathrm{rad})}=0$ whose equations of state mimic the one for radiation. As these points do not correspond to any known matter, they are not physically interesting. Hence, we discard these solutions in Subsection III C as non–physical ones.

  The point P_4 is a special case of P_2 if m is set to be $m=-1$, and its eigenvalues are found to be

$$-5, \quad -3, \quad 4(1+\frac{1}{m}), \quad -\frac{3}{2}. \tag{3.33}$$

  When $-1<m<0$, the point P_4 is a stable point, and is a saddle one otherwise. This property has the same features in the $f(R)$ gravity.

  The point P_5 is a new solution, which does not appear in the $f(R)$ gravity. The eigenvalues are derived as

$$-\frac{7}{2}, \quad -\frac{3}{2}, \quad \frac{m(5+11m)-5r(1+r)m'-5c(m,m')}{4m^2}, \quad \frac{m(5+11m)-5r(1+r)m'+5c(m,m')}{4m^2}, \tag{3.34}$$

  where

$$c(m,m')\equiv\left\{m^2(1+m)^2+rm'\Big[-2m(1+m)+2(-1+m)mr+r(1+r)^2m'\Big]\right\}^{1/2}. \tag{3.35}$$

  As it is obvious, the point P_5 never becomes unstable. When m is a non–zero constant, we have the eigenvalues as

$$-\frac{7}{2}, \quad -\frac{3}{2}, \quad \frac{3}{2}, \quad 4+\frac{5}{2m}, \tag{3.36}$$

  i.e., P_5 is a saddle point for constant m. When $m\to 0$, the eigenvalues become

$$-\frac{7}{2}, \quad -\frac{3}{2}, \quad -\frac{5m'}{2m}, \quad \frac{5}{2m}. \tag{3.37}$$

  Therefore, when $m\to 0^-$ with $m'<0$, this point is a stable one, otherwise is a saddle one.

  The last point in this category is P_7, which is regarded as a special case of the point P_2 for $m=1/4$. This point has eigenvalues

$$\frac{7}{2}, \quad 2, \quad \frac{m(-1+9m)+r(1+r)m'-c(m,m')}{2m^2}, \quad \frac{m(-1+9m)+r(1+r)m'+c(m,m')}{2m^2}. \tag{3.38}$$

  Thus, P_7 cannot be a stable point. When m is a non–zero constant, eigenvalues (3.38) read

$$\frac{7}{2}, \quad 2, \quad 4-\frac{1}{m}, \quad 5, \tag{3.39}$$

  i.e., for $0<m<1/4$, the point P_7 is a saddle point, and otherwise, it behaves as an unstable point. In the limit $m\to 0$, the eigenvalues behave as

$$\frac{7}{2}, \quad 2, \quad -\frac{1}{m}, \quad \frac{m'}{m}, \tag{3.40}$$

  where for $m\to 0^-$ and $m'<0$, this point is unstable, and otherwise, is a saddle point.

- The Point P_6

  This is a point with an unusual feature. The value of the density parameter $\Omega^{(\mathrm{m})}$ does not match the equation of state in a meaningful manner, for we have $w^{(\mathrm{eff})}=1/3$ and $\Omega^{(\mathrm{m})}=2$. However, in this model, in the evolution of universe and dependent on the stability of this point, it may occur that universe approaches to this point. Hence, like the points P_4, P_5 and P_7, the stability of this point should be considered. The eigenvalues are given by

$$-2, \quad \frac{3}{2}, \quad \frac{m(1+7m)-r(1+r)m'-c(m,m')}{2m^2}, \quad \frac{m(1+7m)-r(1+r)m'+c(m,m')}{2m^2}. \tag{3.41}$$

  The first two eigenvalues, -2 and $3/2$, show that this point is always a saddle one for all values of m and m'.

- The Point P_8

  The point P_8 is the only de Sitter fixed point of minimally–coupled form of $f(R,T)$ gravity. The corresponding eigenvalues are represented as

$$-3, \quad -\frac{3}{2}, \quad \frac{1}{2}\Big(-3-\sqrt{25-\frac{16}{m}}\,\Big), \quad \frac{1}{2}\Big(-3+\sqrt{25-\frac{16}{m}}\,\Big). \tag{3.42}$$

  This point is a stable one in the range $0<m<1$, and otherwise, is a saddle point.

Table 2. The stability of the fixed points in both $f(R,T)$ and $f(R)$ gravities without radiation.

Fixed point	Stability in $f(R,T)$ gravity	Stability in the $f(R)$ gravity
P_1	$a)\ \forall\ m,\ m'>-1,$ Saddle $b)\ 0<m<1/2,\ m'<-1,$ Stable $c)\ m\to\pm\infty,\ \forall\ m',$ Saddle	Does not appear
P_2	$d)\ 0<m<1/4,\ m'>-1,$ Unstable $e)\ m<-1/2(1+\sqrt{3}),\ m'>-1,$ Stable $f)\ -1/2<m<0,\ m'>-1,$ Stable $g)\ m>1,\ m'>-1,$ Stable $h)\ 1/2<m<1,\ m'<-1,$ Stable $i)\ m\to\pm\infty,\ m'>-1,$ Stable	The same properties except for $h)\ (1/2)(-1+\sqrt{3})<m<1,\ m'<-1,$ Stable
P_3	Always is a Saddle point	$j)\ 0<m<0.327,\ m'>-1,$ Saddle $k)\ \forall\ m,\ m'=0,$ Saddle
P_4	$l)-1<m<0,$ Stable; otherwise Saddle $m)\ P_4=P_2\ _{\lvert m=-1}$	The same properties
P_5	$n)\ \forall m,\ m'=0,$ Saddle; otherwise Saddle or Stable $o)\ m\to 0^-,\ m'<0,$ Stable; otherwise Saddle	Does not appear
P_6	Always is a Saddle point	$p)\forall\ m,\ m'=0,$ Saddle; otherwise Saddle or Stable
P_7	$q)\ \forall\ m, m'\neq 0,$ Saddle or Unstable $r)\ 0<m<1/4,\ m'=0,$ Saddle; otherwise Stable $s)\ m\to 0^-, m'<0,$ Unstable; otherwise Saddle $t)\ P_7=P_2\ _{\lvert m=1/4}$	The same properties
P_8	$u)\ 0<m<16/25,\ r=-2,$ Spiral Stable $v)\ 16/25\leq m<1,\ r=-2,$ Stable $w)$ Otherwise Saddle	The same properties

B. Effects of Radiation

In this subsection, we take into account the effects of radiation for the fixed points, and particularly check any possible change in the stability of the fixed points[17] $P_1,\ P_2,\ P_3$ and P_8.

[17] As discussed before, the points P_4–P_7 do not have physical meaning and hence, we do not consider them in this subsection.

The existence of radiation adds two new fixed points P_9 and P_{10}, as shown in Table 1. The point P_9 is a standard radiation point with the eigenvalues $(4, 4, 5/2, -1, 1)$, which denotes that this point is always a saddle point the same as in the $f(R)$ gravity.

The eigenvalues of P_{10} are given as

$$\frac{5}{2}, \quad 1, \quad \frac{m-1+\sqrt{81m^2+30m-15}}{2(m+1)}, \quad \frac{m-1-\sqrt{81m^2+30m-15}}{2(m+1)}, \quad 4(1+m'). \tag{3.43}$$

It is interesting that the point P_{10} is always a saddle one irrespective of the values of m and m', for, numerically, it is impossible that the third and forth eigenvalues simultaneously take positive values. Furthermore, P_{10}, in the limit $m \to 0$, gives another radiation fixed point, in which the eigenvalues are non–singular, i.e. they are achieved as

$$\frac{5}{2}, \quad 1, \quad \frac{-1+i\sqrt{15}}{2}, \quad \frac{-1-i\sqrt{15}}{2}, \quad 4(1+m'), \tag{3.44}$$

where m' must be evaluated at $r \to -1$.

The inclusion of radiation does not change the stability properties of the eigenvalues of the other fixed points. In fact, the addition of radiation to the action leads to the appearance of the values $-5/2$, $(2-4m-10m^2)/[m(1+2m)]$, -1 and -4 as the fifth eigenvalues of P_1, P_2, P_3 and P_8, respectively. Thus, it is obvious that none of the stability properties of the accelerated fixed points and the matter point P_3 do change. This means that all the cosmological solutions which have a true sequence $P_3 \to P_{1,2,8}$ can include a saddle radiation era for $m \to 0^+$.

C. Cosmological Solutions

"Good" cosmological solutions are those that pass a long enough matter dominated era followed by an accelerated expansion, hence, any matter point contained in the model must be a saddle point in the phase space. However, the eras that show the accelerated expansion should be an attractor (a stable point) in the phase space. In this study, the only point that involves a matter point is P_3 for $\mid m \mid \to 0^+$, and P_1, P_2, P_3 and P_8 can be the accelerated points. Hereafter, we indicate the matter point P_3 with the condition $m(r \approx -1) \to 0$ as $P_3^{(0)}$. It is worth mentioning that any well–defined curve $m(r)$ of each model must satisfy the relations $m(r_i) = -r_i - 1$ and $\mathcal{M}(r_i) = 0$ for some root r_i, the second condition is equal to the first one for cases containing $m(r_i) \neq 0$. The equation $m(r_i) = -r_i - 1$ gives some roots that belong to the points P_1, P_2 or P_3 which we generally indicate as $P_{1(a,b,\cdots)}$, $P_{2(a,b,\cdots)}$ or $P_{3(a,b,\cdots)}$.

The accelerating roots of P_3 labeled by $a, b, \cdots$ correspond to some negative matter density parameters as are shown in Subsection III A and therefore, cannot be a physical one, hence, we discard them. Consequently, we should consider the cosmological transitions of $P_3^{(0)}$ to either P_1, P_2 or P_8. Another assumption that we apply in the rest of this work is to discard solutions with $m \to 0^-$, for from (3.30), it is obvious that one of the eigenvalues gets a large positive value for small negative value of m and hence, diverges for infinitesimal negative values. This means that, the trajectories leave the matter era very fast and hence, the matter era becomes very short which causes difficulties in matching the model with the observations. Thus, in general, the models with $m \to 0^-$ are unacceptable. We indicate in the following classification that, as P_3 is a saddle point irrespective of the values of m and m', there are more cosmological solutions than in the $f(R)$ gravity. We study these transitions in turn, and suppose that there are some roots in all important regions for the generality of the discussion. Also, we assume that the condition $m(r_i) = -r_i - 1$ holds with $m(r_i) \neq 0$.

- $P_3(m'_3 > -1, m > 0)$ and $P_3(m'_3 < -1, m > 0)$ to $P_1(m'_1 < -1, m > 0)$[18]

  The point P_1 is a stable one in the range $0 < m < 1/2$ provided that $m'_1 < -1$, whilst P_3 is always a saddle point. The curve $m(r)$ must intersect[19] the line $m = -r - 1$ with a derivative $m'_3 > -1$ or $m'_3 < -1$ for leaving the matter epoch, and entering the accelerated epoch with $m'_1 < -1$. Theoretically, the transition $P_3(m'_3 > -1, m > 0)$ to $P_1(m'_1 < -1, m > 0)$ is possible as is shown in Figure 1 labeled Class I solutions. However, the transition from $P_3(m'_3 < -1, m > 0)$ to $P_1(m'_1 < -1, m > 0)$ is not possible, these solutions are labeled as Class VII_a in Figure 2. Nevertheless, there is a special case, namely, when P_3 and P_1 are solutions of the model with the same root r, in which one has $m'_{1,3} < -1$. Hence, it demonstrates an acceptable cosmological solution, and we indicate this type of solution as Class II (Figure 1).

---

[18] We define $m'_i \equiv m' \mid_{P_i}$.

[19] Since the assumption $g'(R) > 0$ leads to a monotonic function $r(R)$ and then, a single valued $m(r)$, hence, we do not consider a multivalued $m(r)$.

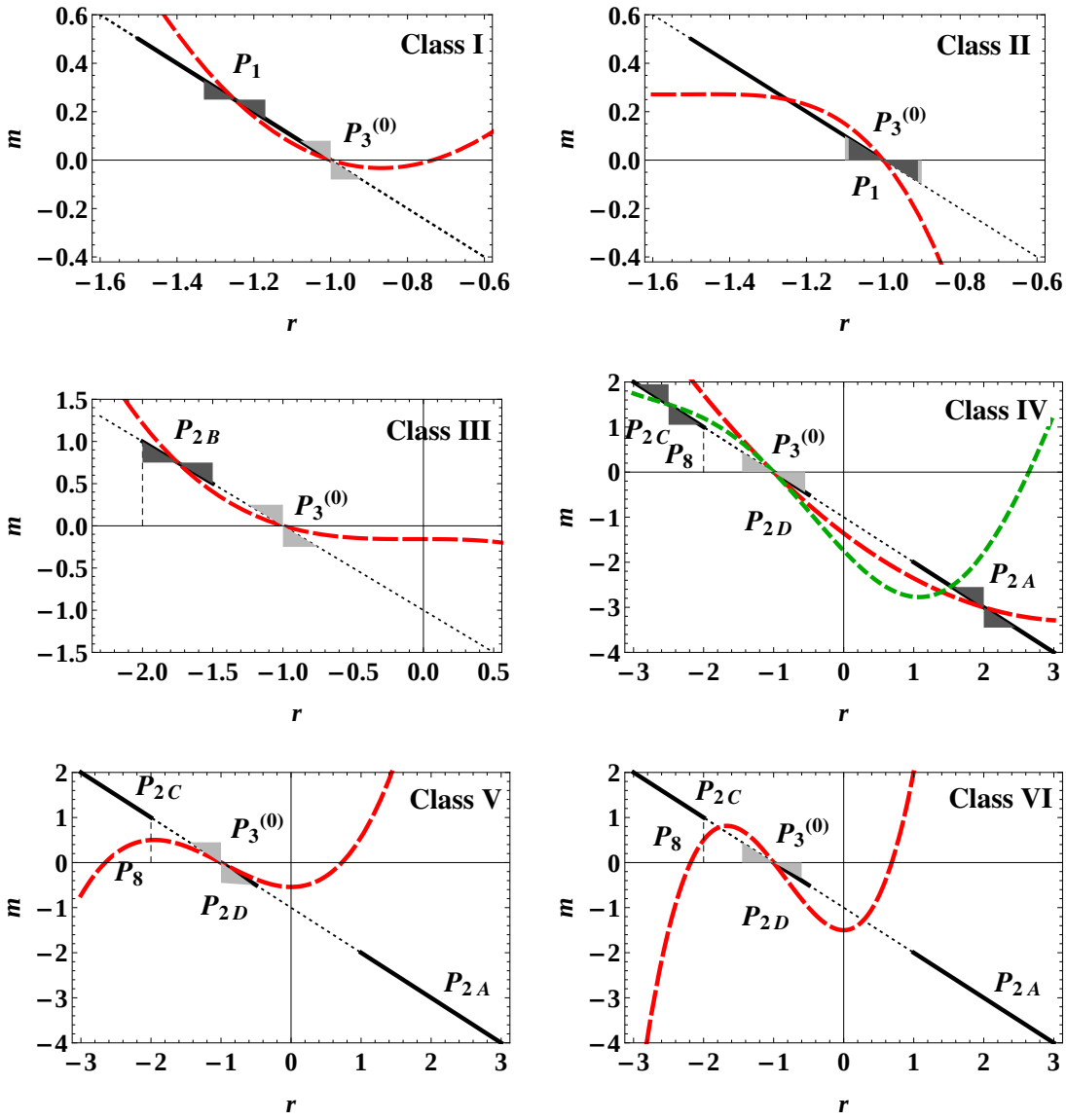

Figure 1. (color online). **Acceptable cosmological solutions of $f(R,T)=g(R)+h(T)$ gravity.** The classification of $f(R,T)$ model in the (r,m)–plane. The line $m=-r-1$ and different curves of $m(r)$, for the six classes of acceptable cosmological solutions, are plotted. The transitions are depicted from the matter epoch $P_3^{(0)}$ to the accelerated point P_1 in Classes I and II, to the accelerated point P_2 in Classes III and IV, and to the de Sitter point P_8 in Classes V and VI. The matter–acceleration epoch transition occurs in Class II for the same value of r, and in Class VI, before reaching to the de Sitter point P_8, with a non–stable acceleration middle stage. The solutions are permitted only in the black solid regions on the line $m=-r-1$ provided that $m_1'<-1$, and $m_{2,\mathcal{A},\mathcal{D},\mathcal{C}}'>-1$. For P_3, we can have either $m_3'<-1$ or $m_3'>-1$ depending on the corresponding class. In Classes I, II and V, we have $m_3'>-1$ whilst in the rest, we have $m_3'<-1$. Unallowable slopes for the curve $m(r)$ are indicated by the light gray triangles for $P_3^{(0)}$ (actually, there is no unallowable slope for $P_3^{(0)}$, however, the light gray triangles are indicated for the sake of classification) and by the gray ones for P_1 and P_2. The dashed curves show hypothetical curves which intersect the line $m=-r-1$ in the critical points P_1, P_3 and P_2 in the regions $\mathcal{A}$, $\mathcal{D}$ and $\mathcal{C}$. All of the classes of solutions are new ones in $f(R,T)$ gravity except for Classes III and V which also appear in the $f(R)$ gravity.

- $P_3(m_3'>-1, m>0)$ to $P_2(m_2'>-1)$ in Regions $\mathcal{A}$, $\mathcal{D}$, $\mathcal{C}$ and to $P_2(m_2'<-1)$ in Region $\mathcal{B}$

  This class includes two classes of solutions. In the first class, there is no connection between $P_3^{(0)}$ and P_2 in the regions $\mathcal{A},\mathcal{D}$ and $\mathcal{C}$, which we call them as Class VII_b drawn in Figure 2. All solutions with whether an improper transition (transition from unallowable regions) or without connection with the matter point $P_3^{(0)}$ fall in this class. In the second class, it is possible to connect $P_3^{(0)}$ with $m_3'>-1$ to P_2 with $m_2'<-1$ in the region $\mathcal{B}$ which we depict an example of these solutions in Figure 1 labeled as Class III solutions. Note that, these

classes of solutions also appear in the $f(R)$ gravity.

- $P_3(m'_3 < -1, m > 0)$ to $P_2(m'_2 > -1)$ in Regions $\mathcal{A}$, $\mathcal{D}$, $\mathcal{C}$ and to $P_2(m'_2 < -1)$ in Region $\mathcal{B}$

  Since P_3 is a saddle point irrespective of the value of m', it can be connected to the point P_2 in the regions $\mathcal{A}$, $\mathcal{D}$ and $\mathcal{C}$ in which the solutions are illustrated as Class IV in Figure 1. On the other hand, because we have $m'_{2,3} < -1$ in the region $\mathcal{B}$, there is no possibility to connect $P_3^{(0)}$ to P_2 in this region, these solutions are classified as Class VII_c in Figure 2.

- $P_3(m'_3 > -1, m > 0)$ and $P_3(m'_3 < -1, m > 0)$ to $P_8(0 < m(r = -2) < 1)$

  In this last class, there are two situations that can lead to a stable accelerated epoch. In the first one, after leaving the matter point, the trajectories go to the final attractor at the point P_8, and we refer to them as Class V (Figure 1). However, in the latter one, before reaching at the final attractor, there is a "false" accelerating era in which the curve $m(r)$ does meet the line $m = -r - 1$ in an unallowable region of the point P_1, in which there is no stable accelerated expansion. These solutions are labeled as Class VI (Figure 1).

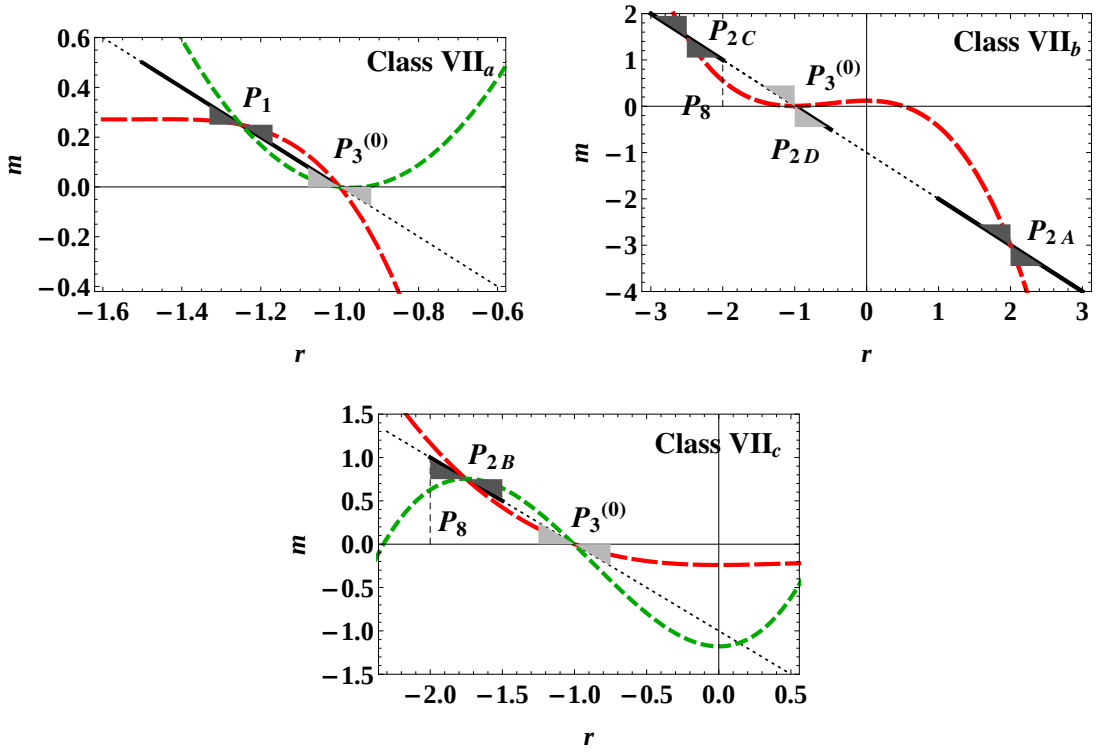

Figure 2. (color online). **Unacceptable cosmological solutions of $f(R,T) = g(R) + h(T)$ gravity.** Some classes of solutions, that suffer from either the absence of a matter dominated epoch or a stable accelerated era or unallowed transitions from matter to acceleration phase, are presented. There may be some other classes related to these solutions, but all of them can be accounted as subclasses of the mentioned ones. Again, as in Figure 1, the dashed curves show hypothetical curves which intersect the line $m = -r - 1$.

IV. CASE STUDIES

In this section, without loss of generality, we examine the discussed classification scheme by considering some well–defined specific theories for simplicity and then, investigate the possible cosmological solutions. First of all, by "well–defined", we mean the corresponding models whose $m(r)$ curves can be derived explicitly with respect to r. We do not go into the details unless there would be some new cosmological solutions with respect to the $f(R)$ gravity,

though to complete the discussion, we may mention the other solutions wherever it is necessary. As the related models are determined by the behavior of their curves $m(r)$, our task is to find the cosmological solutions by exploring the properties of these curves. The following discussed theories are of form $f(R,T)=g(R)+\sqrt{-T}$, where the functionality of $\sqrt{-T}$ is enforced by the conservation law, equation (3.6). As mentioned in Refs. [83, 84], some $f(R)$ gravity models cannot pass the necessary criteria in order to have an acceptable cosmological history, e.g., the lack of a deceleration expansion period to admit a standard structure formation [85], or a quick transition from radiation era to the late–time acceleration or the lack of a connection between matter era and the late–time acceleration era. In this respect, the authors of Refs. [76, 83, 84] have shown that theories of the form $f(R)=\alpha R^n$ and $f(R)=R^p\exp(qR)$ do not lead to a connection between the standard matter era and accelerated attractors. In addition to these difficulties, the authors of Ref. [76] have numerically shown that the models of type $f(R)=R^p[\log(\alpha R)]^q$ and $R^p\exp(q/R)$ suffer from a non–standard matter era for some initial values. In the former one, the matter era is not effectively dominant and in the latter one, the standard matter era is replaced by the ϕMDE epoch.[20] Hence, we reconsider the following plausible models in the background of $f(R,T)$ gravity, in order to find out whether these issues can be cured. Incidentally, for m as a constant parameter, definition (2.20) gives $g(R)\propto R^{m+1}$, i.e. a power–law function. Finally, at the end of this section, we briefly furnish the comparison of the properties of solutions for the investigated models in both $f(R,T)$ and $f(R)$ gravities in Table 3.

A. $f(R,T)=aR^{-\beta}+\sqrt{-T}, \quad a>0, \quad \beta\neq 0$

This theory gives $m(r)=-\beta-1$, which intersects the line $m=-r-1$ at $r=\beta$. As $m(r)=0$ is valid only for $\beta=-1$, hence, the condition $\mathcal{M}(r)=0$ must be satisfied for all values of β except for $\beta=-1$. In this case, because we have $x_3=\beta x_2$, the system reduces to a system with three degrees of freedom, in which the eigenvalues of the points P_1 and P_3 are given by the first three values in (3.19) and (3.28), respectively. To be more exact, P_1 is accelerated in $-1.50<\beta<-1.43$ and $-1.43<\beta<-1$, where in the first range, we have a stable accelerated epoch, and the second one determines a spiral stable accelerated epoch. On the other hand, for $-1.43<\beta<-1$, this theory has a saddle matter era with a damped oscillation when $m\to 0^+$, and for the same root, P_1 is a spiral stable accelerated point which means the corresponding models belong to Class II for categorization purposes. Therefore, in the background of $f(R,T)$ gravity, this theory has a cosmological solution with a standard matter–acceleration epoch sequence unlike the $f(R)$ gravity. We illustrate three examples of this theory in Figure 3 with the same initial values except x_3. In this case, r has a constant value with respect to the time. The diagrams show some disturbances originating from the deviation of the magnitude of β from one, i.e., as $|\beta|$ deviates from one, more disturbances occur. The reason is that the increase of the magnitude of β leads to the growth of the deviation of m from zero, and this causes the increment in the error of matter and radiation solutions of the system of equations (3.8)–(3.11) in turn. The diagrams smooth by decreasing in the deviation, showing an appropriate succession of the radiation–matter–accelerated expansion eras. These examples have the point P_1 as an attractor solution with $-0.65<w^{(\mathrm{eff})}<-0.5$. The diagrams are made in order to have the present values $\Omega_0^{(\mathrm{m})}\approx 0.3$ and $\Omega_0^{(\mathrm{rad})}\approx 10^{-4}$.

B. $f(R,T)=R^p\exp(qR)+\sqrt{-T}, \quad q\neq 0$

In this theory, for $r\neq 0$, we get $m(r)=-r+p/r$, $\mathcal{M}(r)=(p+r)/(p-r^2)$ and $m'(r)=-1-p/r^2$ which are independent of q. For $r=-p$, the corresponding models do not satisfy the condition $\mathcal{M}(r)=0$ for $p=0$ and $p=1$, however, for the other values of p, the two conditions hold. On the other hand, for $p\approx 0$, we have $m(r)\approx -r$, hence, the condition for the existence of a matter solution, $m(r\approx -1)\approx 0^+$ is not met and therefore, the pure exponential models do not have any cosmological solution. Nevertheless, in addition to $\mathcal{M}(r)\approx 0$, in order to have $m\to 0^+$, the condition[21] $r\approx -p$ for $p\to 1^+$ must hold. Actually, for this theory, we have $r=-1-qR$, hence, we get $r\to -1$ from the left–hand side only when $R\to 0^+$ with $q>0$. Since $m_3'(p\to 1^+)<-1$ and $m_1'(-3/2<r<-1)<-1$, it is impossible to connect $P_3^{(0)}$ to P_1 for two different roots of $m(r_i)=-r_i-1$. One exception occurs when P_1 for the same root is the attractor solution, thus in such a case, there is a cosmological solution which belongs to Class II. In Figure 9, in the (r,m)–plane, we draw a plot for the $m(r)$ curve for this theory with $p=1.001$. Also, to illustrate the idea, we numerically depict interesting cosmological quantities predicted by this theory in Figure 4 for $p=1.001$ and the initial value $r_i=-1.002$ in order to have the present values $\Omega_0^{(\mathrm{m})}\approx 0.3$ and $\Omega_0^{(\mathrm{rad})}\approx 10^{-4}$.

---

[20] The ϕ–matter–dominated–epoch (ϕMDE) has been introduced in Ref. [86].
[21] More precisely, $r\to -1^-$.

C. $f(R,T) = R + \alpha R^{-n} + \sqrt{-T}, \quad n \neq 0$

For this theory, we obtain $m(r) = -n(1+r)/r$ and $\mathcal{M}(r) = 1 - r/n$,[22] which show that the condition $\mathcal{M}(r) = 0$ is satisfied only for $r = n$, that in turn gives $m \neq 0$. On the other hand, the corresponding models contain the matter point $P_3^{(0)}$ when $r = -1$, which means that only models with $n = -1$ can be accepted. However, we describe the properties of solutions for the values of n approaching -1 in the following models (where in these cases we have $\mathcal{M}(r = -1) \approx 0$).

- Models With $n \to -1^-$

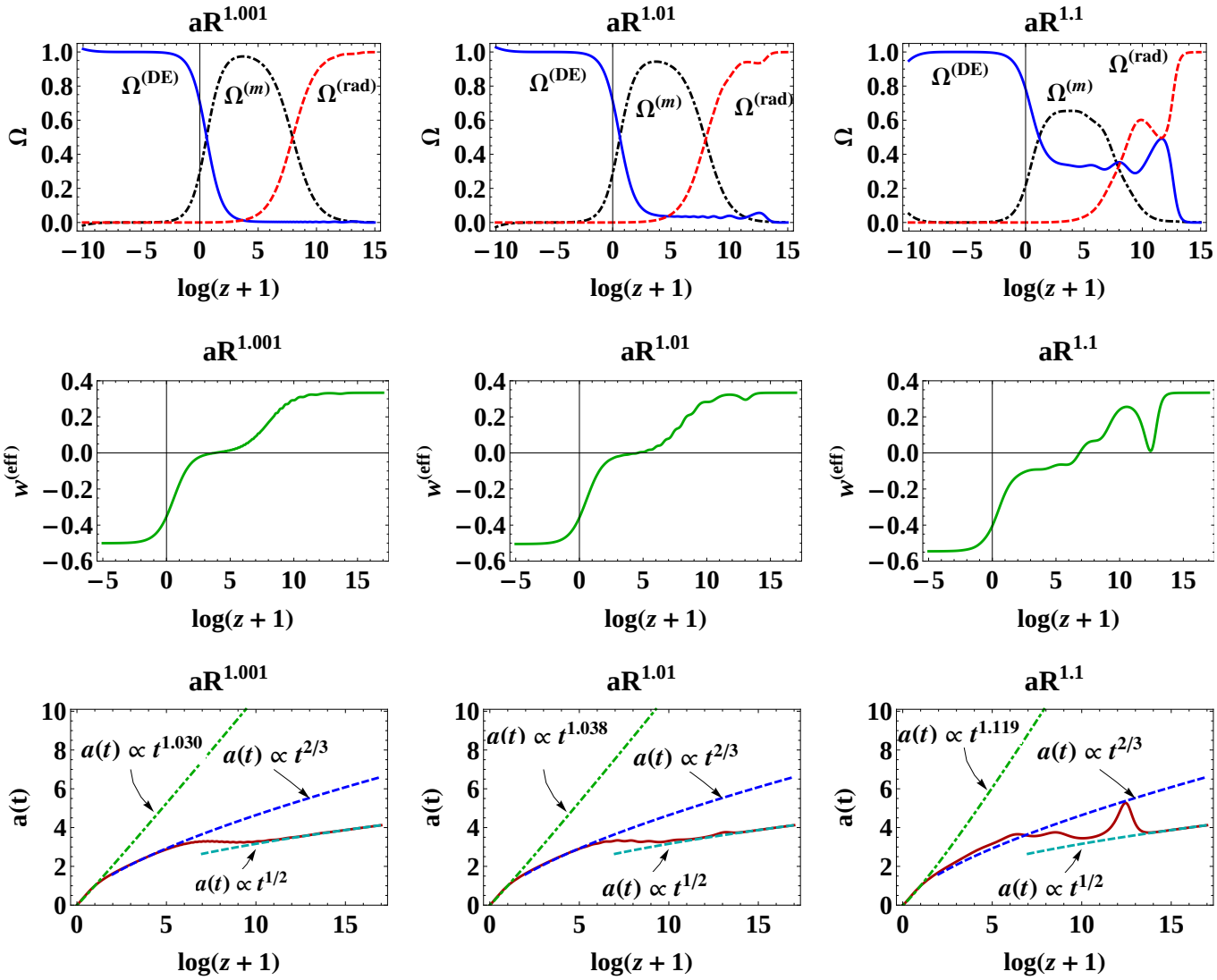

Figure 3. (color online). **Cosmological solutions of $f(R,T) = aR^{-\beta} + \sqrt{-T}$ gravity.** The numerical solutions with $a > 0$ for three values of β are presented. The density parameters for various ingredients are plotted in the first row, the effective equation of state parameter in the second row and the evolution of scale factor in the last row. The diagrams are plotted for the initial values $x_1 = 10^{-4}$, $x_2 = -10^{-4}$, $x_3 = -\beta \times 10^{-4}$, $x_4 = 10^{-13}$ and $x_5 = 0.999$ corresponding to $z \approx 2.42 \times 10^7$. The diagrams are made to be consistent with $\Omega_0^{(\mathrm{m})} \approx 0.3$ and $\Omega_0^{(\mathrm{rad})} \approx 10^{-4}$ at the present epoch, however, they give $-0.65 < w^{(\mathrm{eff})} < -0.5$ instead of $w^{(\mathrm{eff})} \to -1$. The peak of $\Omega^{(m)}$ decreases with the increment in β, i.e., as β increases the diagrams get tangled up. Such disorderings are indicated in the diagrams of $w^{(\mathrm{eff})}$ and in the deviations of the behavior of the scale factor in the matter epoch from its standard form $a \propto t^{2/3}$. The best solutions are achieved for $\beta \to -1$.

[22] In obtaining the equation $\mathcal{M}(r) = 1 - r/n$, we assume $r \neq -1$; however, after removing the ambiguity at $r = -1$, it gives $\mathcal{M}(r = -1) = 1 + 1/n$.

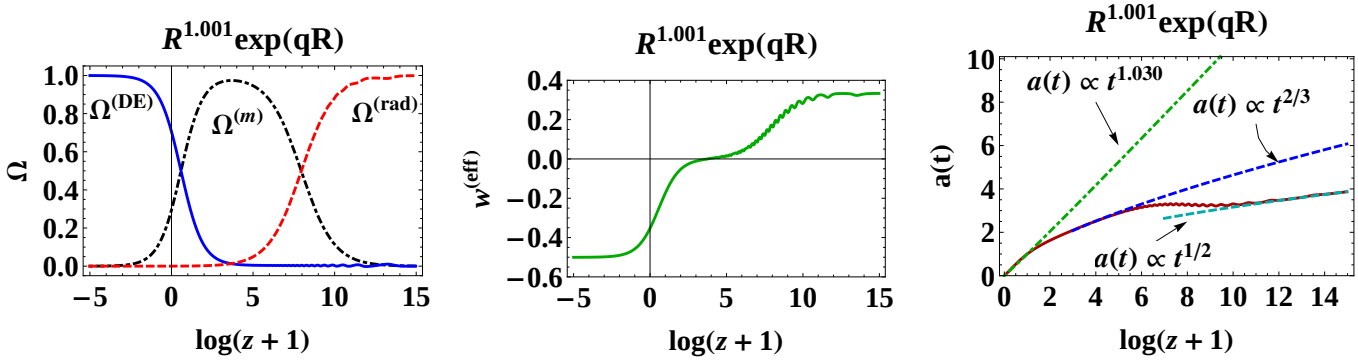

Figure 4. (color online). **Cosmological solutions of $f(R,T) = R^p \exp(qR) + \sqrt{-T}$ gravity.** The plots are presented for $p = 1.001$ and the initial values $x_1 = 10^{-4}$, $x_2 = -10^{-4}$, $x_3 = 1.002 \times 10^{-4}$, $x_4 = 3.8 \times 10^{-13}$ and $x_5 = 0.999$ corresponding to $z \approx 3.17 \times 10^6$. The diagram of $w^{(\text{eff})}$ shows that the final attractor solution is P_1. The present values of the density parameters are extrapolated as $\Omega_0^{(\text{m})} \approx 0.3$ and $\Omega_0^{(\text{rad})} \approx 10^{-4}$.

In these cases, the equation $m(r_i) = -r_i - 1$ has two roots, i.e., $r_{1,2} = -1, n$. Generally, we have $m'(r) = n/r^2$, as a result, for the initial values $r_i < \sqrt{|n|}$, we have $m'_3 < -1$ and $m'_1 > -1$, which denote P_1 to be a saddle point. Thus, since $m(r = -2) = -n/2$, these solutions accept the de Sitter point P_8 as the final attractor after a transition from the saddle point P_1. These models belong to Class VI. On the other hand, for $-\sqrt{|n|} < r_i < -1$, the point P_1 is a stable point. These solutions belong to Class II. In Figure 5, we plot the related diagrams of $R + \alpha R^{1.1}$ model. In this example, the initial value $r_i = -1.0008$ is applied in such a way that it chooses P_1 as the final attractor and also gives the present values for the Ω's. Also in Figure 9, we present the $m(r)$ curve for this example.

- Models With $n \to -1^+$

  For models with $n \to -1^+$, the initial conditions $r_i > -\sqrt{|n|}$ are not allowed, for, these conditions lead to $m \approx 0^-$, which is physically ruled out. However, the initial values $r_i < -1$ are allowed and give $m'_1 > -1$. Therefore, in these models, universe after passing a matter dominated stage is trapped in a temporal accelerated expansion state that is determined by P_1 and then, chooses P_8 as a final de Sitter attractor. These models belong to Class VI. In the numerical considerations, we have chosen $r_i = -1.00002$, which results in an acceleration in a transient period by P_1, then a permanent accelerated expansion by P_8; see Figure 5.

In the cases with $n \to -1^-$, cosmological solutions exist only for $\alpha > 0$ in the limit $R \to 0$, whilst the cases with $n \to -1^+$ have solutions provided that $\alpha < 0$ and $R \to \infty$ because $m = n(n+1)\alpha R^{-n-1}/(1 - n\alpha R^{-n-1})$. In the $f(R)$ gravity, these models can have cosmological solutions only when $-1 < n < 0$, however, in $f(R,T)$ gravity, in addition to these solutions, there are acceptable solutions for $n \to -1^-$ as well.

D. $f(R,T) = R^p[\log(\alpha R)]^q + \sqrt{-T}, \quad q \neq 0, \quad \alpha > 0$

This theory has the following functions

$$m(r) = \frac{(p+r)^2 - qr(1+r)}{qr} \qquad \text{and} \qquad \mathcal{M}(r) = \frac{(p+r)^2}{(p+r)^2 - qr(1+r)}, \tag{4.1}$$

where $r \neq 0$. The condition $\mathcal{M}(r) = 0$ holds for $r = -p$, however, only for $p = 1$, we have $m(r) = 0$ for $r = -1$[23] Incidentally, for $p = 1$ and $m(r = -2) = 1 - 1/2q$, the point P_8 is a stable accelerated attractor for $q > 1/2$. Generally, in this theory, there are three situations in which the matter solution $m \to 0^+$ can be obtained, namely,

$$\begin{aligned} &i)\ q > \frac{1+r}{r}, \quad r \to -1^- \Rightarrow \quad m' > -1 \\ &ii)\ q < 0, \quad r \to -1^- \Rightarrow \quad m' < -1 \\ &iii)\ \frac{1+r}{r} < q < 0, \quad r \to -1^+ \Rightarrow \quad m' > -1. \end{aligned}$$

[23] Note that, the existence of the matter point for all types of this case is independent of q.

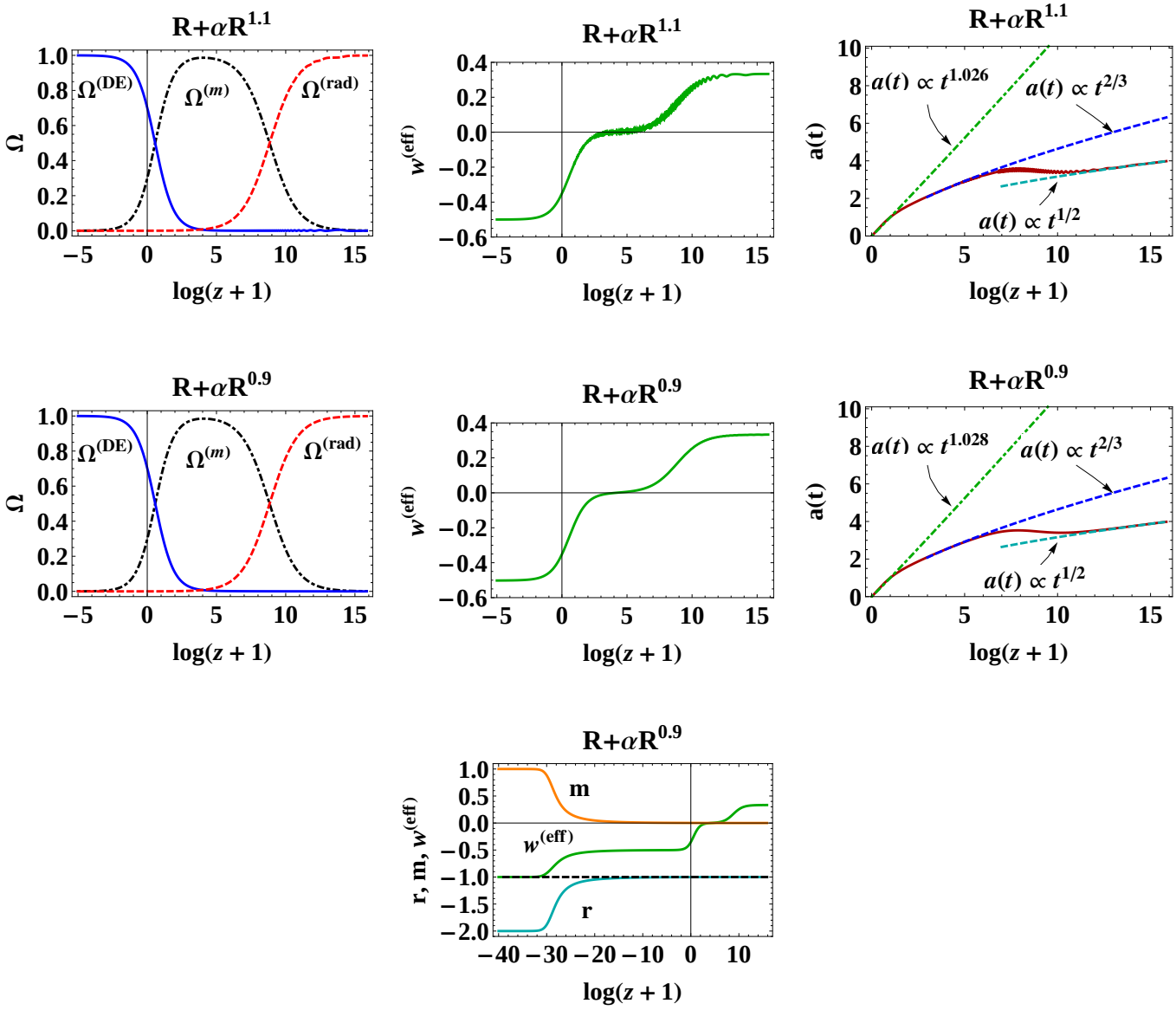

Figure 5. (color online). **Cosmological solutions of $f(R,T) = R + \alpha R^{-n} + \sqrt{-T}$ gravity.** The diagrams are obtained for $n = -1.1$ and the initial values $x_1 = 10^{-4}$, $x_2 = -10^{-5}$, $x_3 = 1.0008 \times 10^{-5}$, $x_4 = 10^{-13}$ and $x_5 = 0.999$ corresponding to $z \approx 7.65 \times 10^6$. Hence, the model matches with the present observational data $\Omega_0^{(\mathrm{m})} \approx 0.3$ and $\Omega_0^{(\mathrm{rad})} \approx 10^{-4}$; however, its $w^{(\mathrm{eff})}$ converges to value -0.5 instead of -1. There are desirable successions of radiation–matter–acceleration phases. The scale factor evolution curve has the asymptotic form of $a \propto t^{1/2}$ at high–redshifts, and behaves as $a \propto t^{2/3}$ when the matter becomes dominant. The model with $n = -0.9$ is plotted for the same initial values except for $x_2 = -10^{-4}$ and $x_3 = 1.00002 \times 10^{-4}$. This model shows a transition from a temporal acceleration epoch to the final attractor in the vicinity of P_8, hence, it belongs to Class VI.

The first situation shows that the corresponding models for $0 < q < 1/2$ with $m'_{1,3} > -1$ lie in Class VII_a. On the other hand, P_2 cannot be the final attractor, for, the curve $m(r)$ does not have any root in the regions $\mathcal{A}$, $\mathcal{B}$, $\mathcal{C}$ and $\mathcal{D}$. However, for $q > 1/2$, the final attractor is P_8. The corresponding models in the second situation, in which $m'_{1,3} < -1$, lie in Class II for the same root r as represented in Figure 5, but the transition to $P_{2\mathcal{B}}$ does not lead to a good cosmological solution, which lies in Class VII_c. In the last situation, the range of q gets narrowed as r approaches to -1, hence, it is of less importance to be studied.

In Figures 6 and 7, we plot two examples of such cases for $q = \pm 1$. The both examples show an acceptable succession of the radiation–matter–accelerated expansion eras. The theory $R \log \alpha R$ belongs to Class VI which has P_8 as the final attractor. In addition to the curves of density parameters for radiation, matter and acceleration eras, the curves of $r \equiv -Rg'/g$, $m \equiv Rg''/g'$ and the effective equation of state are depicted. These curves show a transition from the saddle accelerated point P_1 to a stable de Sitter acceleration expansion phase after a long time. Figure 6 indicates

that the curve $m(r)$ first intersects the line $m=-r-1$ in regions $r\to-1^-$, in which P_1 is a saddle point, then, intersects the line $r=-2$ where P_8 is a stable point. Therefore, these solutions belong to Class VI. Also, $w^{(\rm eff)}$ takes a transition from a non–phantom accelerating era with the value $w^{(\rm eff)}\approx-1/2$ to a de Sitter epoch with $w^{(\rm eff)}\approx-1$. Unlike this theory, the other theory, i.e. $R/\log(\alpha R)$, has P_1 as the only attractor as seen from Figure 6. The latter theory belongs to Class II.

We conclude that the corresponding models of $g(R)=R^p[\log(\alpha R)]^q$ are cosmologically acceptable for $p=1$ with $q<0$ and $q>1/2$ in the background of $f(R,T)$ gravity, whereas in the $f(R)$ gravity, the solutions exist only in the range $q>0$.

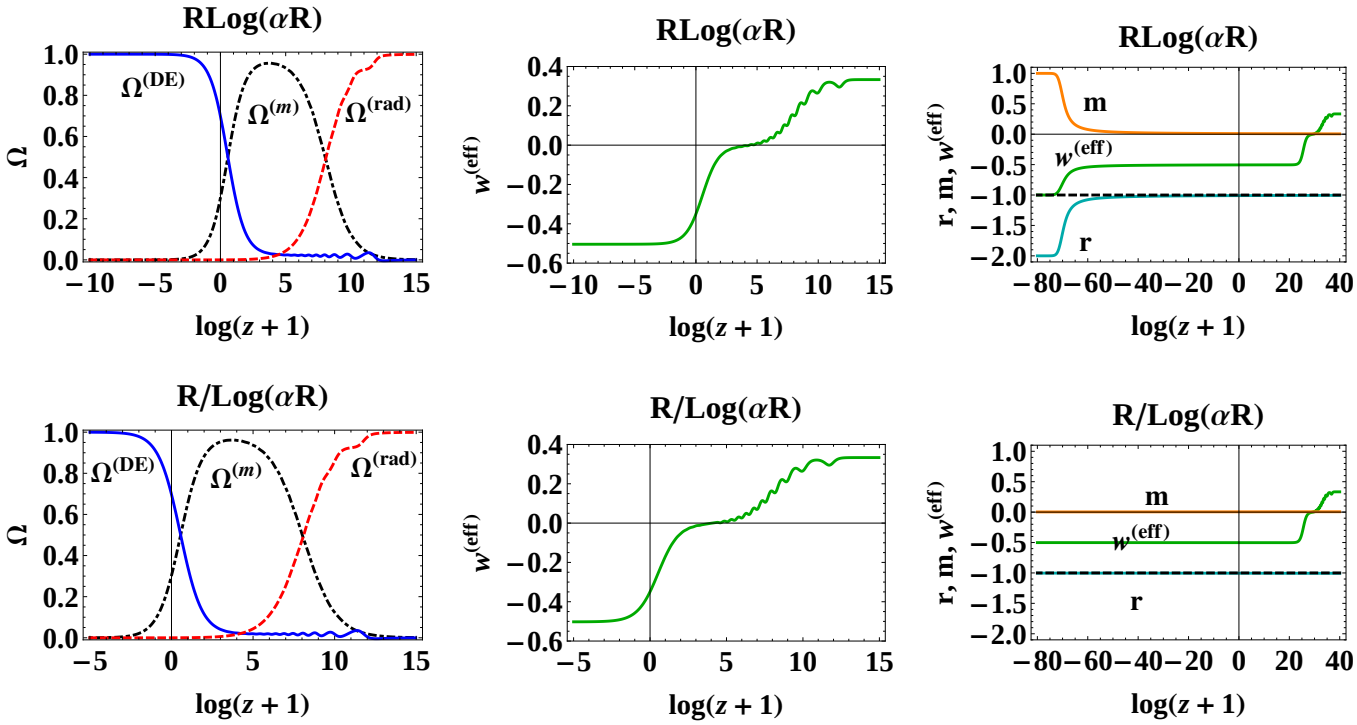

Figure 6. (color online). **Cosmological solutions of $f(R,T)=R(\log\alpha R)^q+\sqrt{-T}$ gravity.** The density parameter and the effective equation of state parameter diagrams are plotted for two values $q=1$ and $q=-1$. The diagrams for m, r and $w^{(\rm eff)}$ are drawn in a wide range of redshift. The Ω's show admissible behaviors in both cases. In the right panel, the first row diagram shows a transition from a saddle accelerated epoch with $w^{(\rm eff)}\approx-0.5$ to a stable one with $w^{(\rm eff)}\approx-1$ for $q=1$. All three diagrams support this result. Unlike $R\log\alpha R$, the theory $R/\log\alpha R$ does not show these transitions. We draw the $m(r)$ curve for the model $R\log\alpha R$ in Figure 9 which indicates that this theory belongs to Class VI. The $m(r)$ curves of the theory first intersect the line $m=-r-1$ in an unallowed region, then the line $r=-2$ as a final attractor. The diagrams are plotted for the initial values $x_1=10^{-10}$, $x_2=-10^{-7}$, $x_3=1.0058\times10^{-7}$, $x_4=4\times10^{-13}$ and $x_5=0.999$ corresponding to $z\approx3.17\times10^6$ for both theories. The diagrams represent the values of $\Omega_0^{(\rm m)}\approx0.3$ and $\Omega_0^{(\rm rad)}\approx10^{-4}$ at the present epoch.

E. $f(R,T)=R^p\exp(q/R)+\sqrt{-T}$

This theory has the relations

$$m(r)=-\frac{p+r(2+r)}{r}\qquad\text{and}\qquad\mathcal{M}(r)=\frac{p+r}{p+r(2+r)},\tag{4.2}$$

where $r\neq0$. The condition $\mathcal{M}(r)=0$ is satisfied when $r=-p$ and for all values of p, except $p=0,1$. On the other hand, the matter era only exists in $r=-p=-1$, hence, we consider the theory in $r=-p$ when $p\to1^+$. In this condition, we have $m_1'>-1$, therefore, the point P_1 cannot be stable whilst P_2 can be a stable accelerated point in the region $\mathcal{C}$. Since $m''(r)=-2p/r^3$, thus the point $(r\approx-1,m\approx0)$ is a minimum with a positive concavity. Note that, for $r<-1$, we have $m(r)<-r-1$, which has an asymptotic behavior in $r\to-\infty$ as $m(r)\to-r$. As in this theory $r=(q/R)-1$, the latter behavior occurs for $q<0$ and $R\to0^+$, which denotes $P_{2\mathcal{C}}$ can be the final attractor. However, the trajectories have already been trapped by P_8 in a finite r. In this theory, like the corresponding models

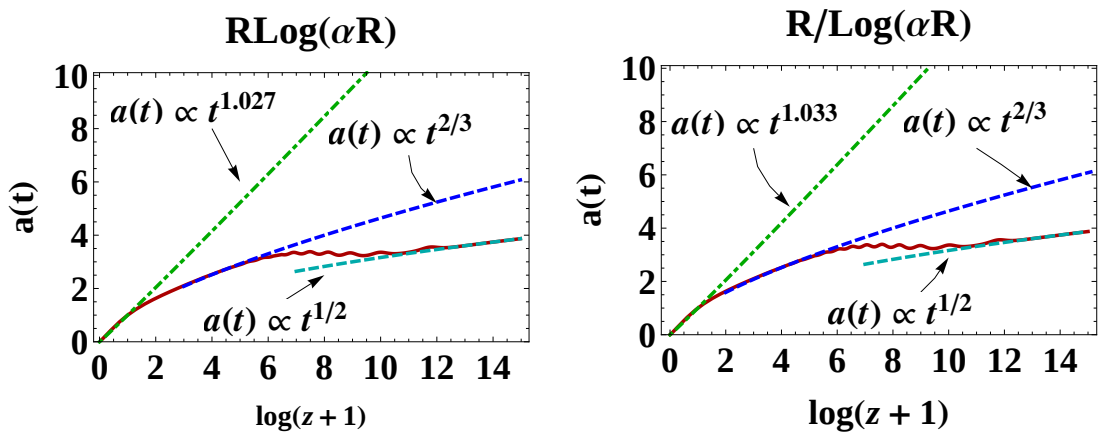

Figure 7. (color online). The scale factor evolution curves for the two theories with $g(R) = R\log\alpha R$ and $g(R) = R/\log\alpha R$ are depicted. The asymptotic lines show the behaviors of the scale factor at the high–redshifts regime, in the matter dominated epoch and at late times.

of $R\log(\alpha R)$, before reaching the final attractor in P_8, there is a short time interval in which the trajectories pass by P_1 (which is a saddle point). Thus, its corresponding models belong to Class VI.

As a result, the corresponding models, in general, have cosmological solutions provided that $q < 0$ for $R \to \infty$. In Figure 8, we depict a numerical calculated example for these models provided we have the present observed values for the density parameters. This example belongs to Class VI, as is obvious by comparing solutions of Class VI (Figure 1) with the corresponding curve $m(r)$ in Figure 9.

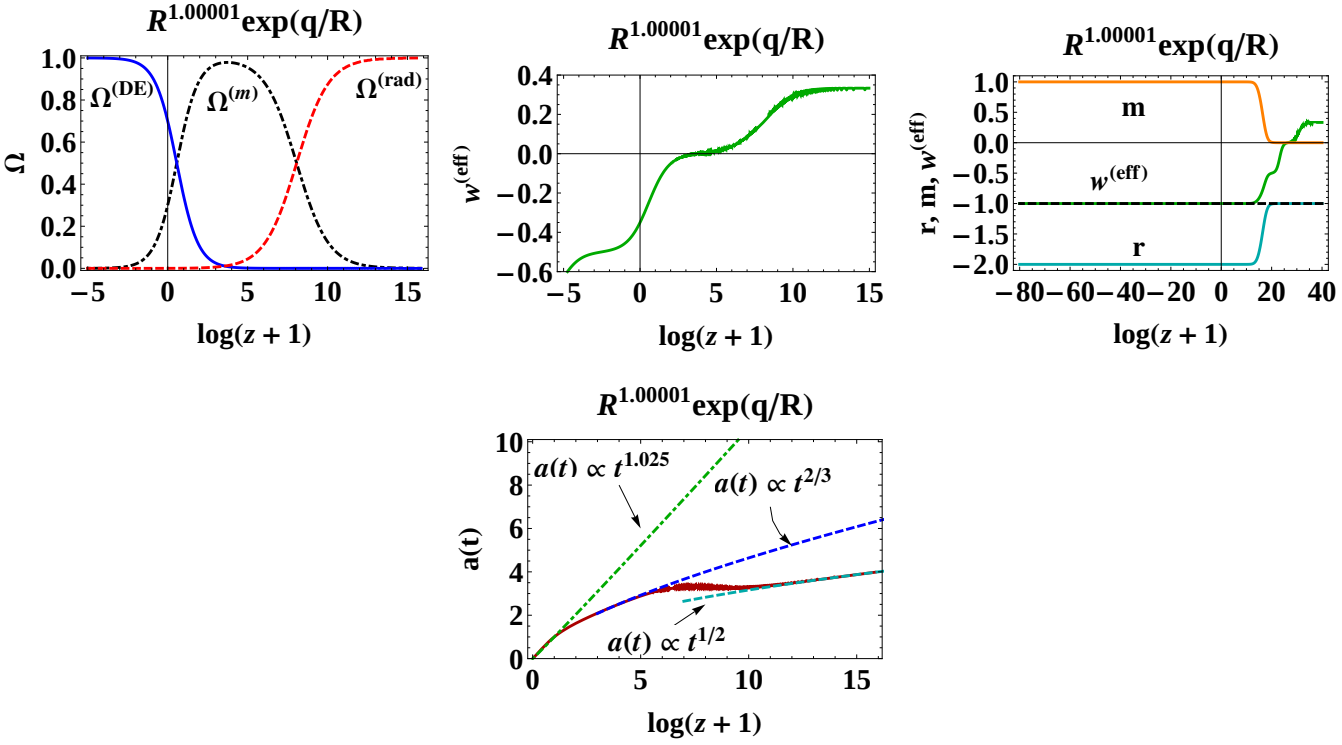

Figure 8. (color online). **Cosmological solutions of** $f(R,T) = R^p \exp(q/R) + \sqrt{-T}$ **gravity.** The plots are provided for $p = 1.00001$ and the initial values $x_1 = 10^{-5}$, $x_2 = -10^{-25}$, $x_3 = 1.00001 \times 10^{-25}$, $x_4 = 10^{-15}$ and $x_5 = 0.9999$ corresponding to $z \approx 3.53 \times 10^7$. In this case, there is always $m_1' > -1$, which denotes P_8 as the final attractor.

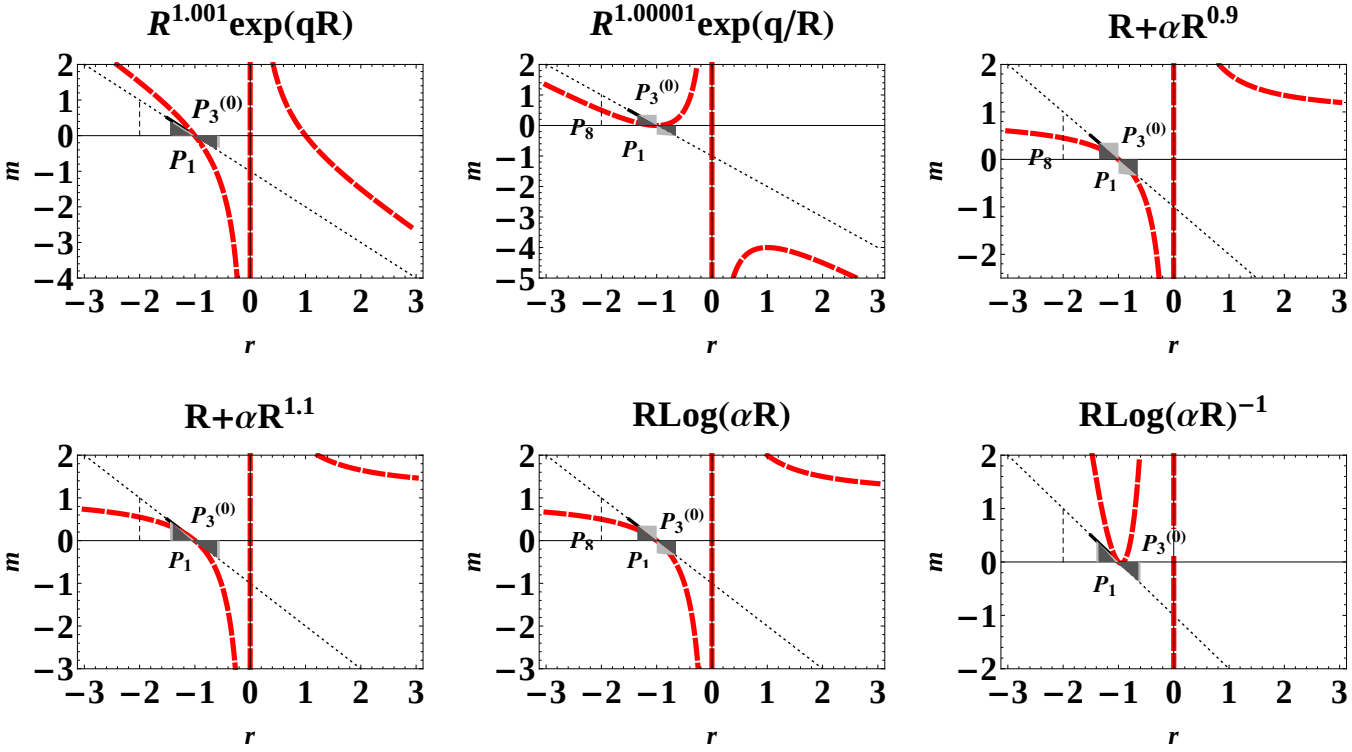

Figure 9. (color online). **Theoretical curves for $m(r)$ for some models in $f(R,T)$ gravity.** The $m(r)$ curves are illustrated for some models corresponding to the represented classifications. Contrary to the $f(R)$ gravity, the existence of the new point P_1 and the new stability condition for P_3 ($P_3^{(0)}$ is a saddle point for both $m' < -1$ and $m' > -1$) bring about the appearance of new acceptable solutions. The models for which P_8 is the final attractor, and are indicated by the two opposite triangles sets, belong to Class V, and those for which P_1 is the final attractor, and are indicated by the two fitted triangles sets, belong to Class I.

Table 3. Cosmological solutions of $f(R,T)$ gravity compared with the $f(R)$ gravity.

Theory	$f(R,T)$ gravity				$f(R)$ gravity	
$g(R)$ Model	Class II	Class VI	Class VII_a	Class VII_b	Class V	Class VII_b
$aR^{-\beta},\ a>0$	$-1.43<\beta<-1$					$-0.713<\beta<-1$
$R^p\exp(qR)$	$p\to 1^+,\ q>0$			$p\approx 0$		$p=0,\ p=1$
$R+\alpha R^{-n}$	$n^{\mathrm{a}}\to -1^-$	$n\to -1^+,\ n\to -1^-$			$-1<n<0,\ \alpha<0$	
$R^p(\log\alpha R)^q$	$p=1,\ q<0$	$p=1,\ q>1/2$	$p=1,\ 0<q<1/2$		$p=1,\ q>0$	$p\neq 1$
$R^p\exp(q/R)$		$p\to 1^+,\ q<0$			$p=1$	$p\neq 1$

[a] For models with $n\to -1^-$, we have $\alpha>0$ and for models with $n\to -1^+$, we have $\alpha<0$.

V. PURE NON–MINIMAL CASE $f(R,T)=g(R)h(T)$

Since we propose to investigate a pure non–minimal case in this section, one should be more careful about the functionality of $h(T)$. Indeed, in the vacuum state, we do not want to have a null Lagrangian. In a loose expression, there should be a solution for the vacuum state (contrary with the strong version of the Mach idea). Therefore, in this non–minimal case, the following assumption is necessary, namely,

$$\lim_{T\to 0} h(T)\neq 0. \tag{5.1}$$

Furthermore, for simplicity, in this and the following sections, we only consider the dust–like matter. Using the definitions presented in Sec. II, from (2.12) and (2.13), we get

$$1+\frac{1}{6}\frac{g}{H^2g'}-\frac{1}{6}\frac{R}{H^2}+\frac{\dot{g'}}{Hg'}+\frac{\dot{h}}{Hh}=\frac{8\pi G\rho^{(\mathrm{m})}}{3H^2g'h}+\frac{gh'\rho^{(\mathrm{m})}}{3H^2g'h} \tag{5.2}$$

and

$$2\frac{\dot{H}}{H^2}+\frac{\ddot{g'}}{H^2g'}+2\frac{\dot{g'}}{Hg'}\frac{\dot{h}}{Hh}+\frac{\ddot{h}}{H^2h}-\frac{\dot{g'}}{Hg'}-\frac{\dot{h}}{Hh}=-\frac{8\pi G\rho^{(\mathrm{m})}}{H^2g'h}-\frac{gh'\rho^{(\mathrm{m})}}{H^2g'h}. \tag{5.3}$$

Rewriting the first equation with respect to the defined variables and parameters (2.14)–(2.16) and (2.23), gives

$$\Omega^{(\mathrm{m})}_{\mathrm{p.n.}}=1-x_1-x_2-x_3-s(3+2x_2), \tag{5.4}$$

where we have defined the corresponding pure non–minimal matter density parameter as

$$\Omega^{(\mathrm{m})}_{\mathrm{p.n.}}\equiv\frac{8\pi G\rho^{(\mathrm{m})}}{3H^2g'h}. \tag{5.5}$$

In the above definition for $\Omega^{(\mathrm{m})}_{\mathrm{p.n.}}$, the existence of the function $h(T)$ warns us about the sign of $\Omega^{(\mathrm{m})}_{\mathrm{p.n.}}$. That is, as we have only adopted that $g'(R)>0$, the density parameter $\Omega^{(\mathrm{m})}_{\mathrm{p.n.}}$ may obtain negative values due to the appearance and functionality of $h(T)$. On the other hand, if one physically demands that $\Omega^{(\mathrm{m})}_{\mathrm{p.n.}}$ must be positive, then, the functionality of $h(T)$ will be restrictive, e.g. an exponential function.

We have three dynamical equations for x_1, x_2 and x_3; the equations for x_2 and x_3 are the same as equation (3.9) and (3.10), respectively. However, the equation for x_1 changes as

$$\frac{dx_1}{dN}=-1+x_1(x_1-x_3)-3x_2-x_3+3s(2x_1-x_3+3s). \tag{5.6}$$

In addition to the EOM constructed by equations (3.9), (3.10) and (5.6), we have a constraint due to the energy–momentum conservation law. It is easy to check that constraint (2.11) leads to the following relations among the parameters n and s with the other variables as

$$n=\frac{x_1x_3}{3mx_2}-\frac{1}{2} \tag{5.7}$$

and

$$s=\frac{x_1x_3}{3mx_2}+\frac{1}{2}, \tag{5.8}$$

which in turn lead to specify the functionality of $h(T)$ and also to make a complicated relation between $g(R)$ and $h(T)$. Indeed, further investigations indicate that $h(T)$ is a complicated exponential function of T, which guaranties that $\Omega^{(\mathrm{m})}_{\mathrm{p.n.}}$ to be positive. Anyway, we have a dynamical system with three variables and two constraints that must hold. This system of equations accepts four fixed points which are summarized in Table 4.

Table 4. The fixed points solutions of $f(R,T)=g(R)h(T)$ gravity without radiation.

Fixed point	Coordinates (x_1,x_2,x_3)	Parameter s	$\Omega^{(m)}_{\mathrm{p.n.}}$	$w^{(\mathrm{eff})}$
P_1	$\left(\frac{m(5-m-a_m{}^{\mathrm{a}})}{4(1+m)},\ -\frac{11+17m+a_m}{8(1+m)^2},\ \frac{11+17m+a_m}{8(1+m)}\right)$	$\frac{1}{12}(1+m+a_m)$	0	$-\frac{7+13m+a_m}{12(1+m)}$
P_2	$\left(\frac{m(5-m+a_m)}{4(1+m)},\ -\frac{11+17m-a_m}{8(1+m)^2},\ \frac{11+17m-a_m}{8(1+m)}\right)$	$\frac{1}{12}(1+m-a_m)$	0	$-\frac{7+13m-a_m}{12(1+m)}$
P_3	$\left(0,\ -\frac{5}{4},\ 2\right)$	0	0	-1
P_4	$\left(-4,\ -\frac{7}{4},\ 0\right)$	0	0	$\frac{1}{3}$

[a] Where, $a_m\equiv\sqrt{-47+38m+121m^2}$.

The most important point that can be observed is that the matter density parameters of all the fixed points are zero. There is no solution to describe a standard matter dominated era. Thus, we do not consider the general properties of their fixed points and henceforth, their stabilities. However, the properties of each point can be briefly summarized. The point P_1 is a non–standard matter era, for, the condition $w^{(\text{eff})} = 0$ is satisfied in $m = -2$, but we have $\Omega^{(m)}_{\text{p.n.}} = 0$. P_1 is a de Sitter point when $m = 0.6$. For this point, the non–phantom accelerating expansion occurs when $0.48 < m < 0.60$, and the phantom accelerating expansion occurs when $m > 0.6$. The point P_2 can expand universe in the range $0.48 < m < 1.40$ in the non–phantom domain and in the range $m < -1$ in the phantom domain. The point P_3 is a special case of the point P_1 when $m = 0.6$, which is a de Sitter point. And, contrary to our initial assumption for the investigation of this theory, the point P_4 resembles a radiation point, which is not physically justified.

VI. NON–MINIMAL CASE $f(R,T) = g(R)\,(1 + h(T))$

Since a general Lagrangian $L = g_1(R) + g_2(R)h(T)$ makes the calculations and the stability considerations more complicated, we will just study the non–minimal case $f(R,T) = g(R)\,(1 + h(T))$.

The following field equations are obtained, namely,

$$1 + \frac{1}{6}\frac{g}{H^2 g'} - \frac{1}{6}\frac{R}{H^2} + \frac{\dot{g'}}{Hg'} + \frac{2\dot{h}}{H(1+2h)} = \frac{8\pi G\rho^{(\text{m})}}{3H^2 g'(1+2h)} + \frac{2gh'\rho^{(\text{m})}}{3H^2 g'(1+2h)} \tag{6.1}$$

and

$$2\frac{\dot{H}}{H^2} + \frac{\ddot{g'}}{H^2 g'} + \frac{\dot{g'}}{Hg'}\frac{4\dot{h}}{H(1+2h)} + \frac{2\ddot{h}}{H^2(1+2h)} - \frac{\dot{g'}}{Hg'} - \frac{2\dot{h}}{H(1+2h)} = -\frac{8\pi G\rho^{(\text{m})}}{H^2 g'(1+2h)} - \frac{2gh'\rho^{(\text{m})}}{H^2 g'(1+2h)}. \tag{6.2}$$

To get the dynamical equation from equations (6.1) and (6.2), we need to define a new variable

$$y \equiv \frac{h}{1+2h}. \tag{6.3}$$

Hence, the corresponding non–minimal matter density parameter satisfies

$$\Omega^{(\text{m})}_{n.} = 1 - x_1 - x_2 - x_3 - 2s(3 + 2x_2)y, \tag{6.4}$$

where

$$\Omega^{(\text{m})}_{n.} \equiv \frac{8\pi G\rho^{(\text{m})}}{3H^2 g'(1+h)}. \tag{6.5}$$

Owing to these variables, the dynamical equations for x_1 and x_4 are derived as

$$\frac{dx_1}{dN} = -1 + x_1(x_1 - x_3) - 3x_2 - x_3 + 6s(2x_1 - x_3 + 3s)x_4, \tag{6.6}$$

$$\frac{dx_4}{dN} = -3sx_4(1 - 2x_4), \tag{6.7}$$

where the corresponding equations for x_2 and x_3 remain unchanged, i.e. equations (3.9) and (3.10). In addition, the parameters n and s are also the same as in equations (5.7) and (5.8), which constrain the variables x_1, x_2 and x_3. The fixed points of this system are represented in Table 5.

In this theory, the point P_1 contains a matter dominated era, and the other points give de Sitter points and the accelerating expansion domains. Nevertheless, it remains to ensure that the matter point is a saddle point, and that we have a stable accelerating point for the late time acceleration of universe. In what follows, we only consider the properties of each fixed point in turn to check these possibilities. More studies on the possible cosmological solutions for some specific models can be carried out; however, this is beyond the scope of this work.

Table 5. The fixed points of theory $f(R,T)=g(R)\,(1+h(T))$ without radiation.

Fixed point	Coordinates (x_1,x_2,x_3,x_4)	$\Omega_{n.}^{(m)}$	$w^{(\rm eff)}$
P_1	$\left(\frac{3m}{1+m},\ -\frac{1+4m}{2(1+m)^2},\ \frac{1+4m}{2(1+m)},\ 0\right)$	$\frac{2-m(3+8m)}{2(1+m)^2}$	$-\frac{m}{1+m}$
P_2	$\left(\frac{2(1-m)}{1+2m},\ \frac{1-4m}{m(1+2m)},\ -\frac{(1-4m)(1+m)}{m(1+2m)},\ 0\right)$	0	$\frac{2-5m-6m^2}{3m(1+2m)}$
P_3	$(-4,\ 5,\ 0,\ 0)$	0	$\frac{1}{3}$
P_4	$(0,\ -1,\ 2,\ 0)$	0	-1
P_5	$\left(\frac{m(5-m-a_m)}{4(1+m)},\ -\frac{11+17m+a_m}{8(1+m)^2},\ \frac{11+17m+a_m}{8(1+m)},\ \frac{1}{2}\right)$	0	$-\frac{7+13m+a_m}{12(1+m)}$
P_6	$\left(\frac{m(5-m+a_m)}{4(1+m)},\ -\frac{11+17m-a_m}{8(1+m)^2},\ \frac{11+17m-a_m}{8(1+m)},\ \frac{1}{2}\right)$	0	$-\frac{7+13m-a_m}{12(1+m)}$
P_7	$(0,\ -\frac{5}{4},\ 2,\ \frac{1}{2})$	0	-1
P_8	$(-4,\ \frac{7}{4},\ 0,\ \frac{1}{2})$	0	$\frac{1}{3}$

- The Point P_1

  This point has the following eigenvalues

$$-\frac{1}{2},\ \frac{-3m+\sqrt{m(256m^3+160m^2-31m-16)}}{4m(1+m)},\ \frac{-3m-\sqrt{m(256m^3+160m^2-31m-16)}}{4m(1+m)},\ 3(1+m'). \quad (6.8)$$

  The point P_1 is a stable point when $m'<-1$ and $0<m<0.346$, and otherwise, a saddle point. If $m'=0$, it will be a saddle point for all values of m. Also, when $m\to 0^+$, it is a saddle point provided that $m'>-1$. This point has a similar property as the corresponding one in the $f(R)$ gravity.

- The Points P_2, P_5 and P_6

  These three points can only play the role of attractor solutions of the system, for, we have $\Omega^{(\rm m)}_{P_{2,5,6}}=0$. The eigenvalues of P_2 are given as

$$-4+\frac{1}{m},\quad \frac{-8m^2-3m+2}{m(1+2m)},\quad \frac{2(1-m^2)(1+m')}{m(1+2m)},\quad \frac{10m^2+3m-4}{6m(1+2m)}. \quad (6.9)$$

  When $m<(-1-\sqrt{3})/2$ or $(-1+\sqrt{3})/2<m<1$, the point P_2 can accelerate the expansion of universe in the non–phantom domain, and when $-1/2<m<0$ or $m>1$, in the phantom domain. There is no stable solution for the phantom accelerating expansion, however, the stable non–phantom accelerating domains are determined by

$$m'<-1,\qquad 0.347\lesssim m<1/2,\qquad -1/3<w^{(\rm eff)}<-0.260. \quad (6.10)$$

  In the limit $m\to 0$, the eigenvalues approximately read as

$$\frac{1}{m},\quad \frac{2}{m},\quad \frac{2}{m}(1+m'),\quad -\frac{2}{3m}, \quad (6.11)$$

  which means that for both $m\to 0^+$ and $m\to 0^-$, this point is a saddle one. Also, in the models with $m'=0$, the point P_2 is a saddle point for all values of m.

  The point P_5 can accelerate the expansion of universe in the non–phantom domain with $-1<w^{(\rm eff)}\lesssim -0.75$ for $0.486\lesssim m<0.6$, and in the phantom domain with $w^{(\rm eff)}<-1$ for $m>0.6$. P_5 is stable in the first range provided that $m'<-1$, and when $m'>-1$ in the second range. Finally, P_6 is always a saddle point in the non–phantom range $0.486\lesssim m<1.4$ and in the phantom range $m<-1$ for all values of m'.

- The Points P_4 and P_7

  The eigenvalues of P_4 are derived to be

$$-3,\quad \frac{1}{2},\quad \frac{1}{2}\left(-3-\sqrt{25-\frac{16}{m}}\right),\quad \frac{1}{2}\left(-3+\sqrt{25-\frac{16}{m}}\right). \quad (6.12)$$

  Clearly, P_4 is a saddle de Sitter point. However, the numerical calculations show that the point P_7 is a stable de Sitter solution for $0<m<1/2$.

We conclude this section with the assertion that the non–minimal coupling Lagrangian $f(R,T) = g(R)\,(1 + h(T))$ can have cosmological solutions in the form of transitions of P_1 to any of the points P_2, P_5 or P_7. Note that, the fixed points P_3 and P_8 have $w^{(\text{eff})} = 1/3$ which means that they are not physically justified in the absence of radiation.

VII. CONCLUDING REMARKS

In this work, we consider the cosmological solutions of $f(R,T)$ theory of gravity for a perfect fluid in a spatially flat, homogeneous and isotropic background FLRW metric via the (r,m)–plane analysis. We include the dust matter and radiation in the action. We investigate some families of this theory that can be written as a combination of a pure function of the trace, e.g., $h(T)$, and a pure function of the Ricci scalar, e.g., $g(R)$, by the virtue of which one would be able to use $f(R,T)$ gravity as a modification of the $f(R)$ dark energy models. In Ref. [76], by introducing two dimensionless parameters r and m, the (r,m)–plane method has been employed to parametrize the $f(R)$ function and simplify the calculations. In this work, we extend their idea to the function $h(T)$ and introduce another two new dimensionless parameters, namely n and s. With these definitions, we consider the cosmological solutions of three general theories with the Lagrangians of minimal, pure non–minimal and non–minimal couplings via the dynamical systems approach. The conservation of the energy–momentum tensor leads to a constraint equation that relates n to the other dynamical variables, and all acceptable cosmological solutions must respect it.

In the minimal gravity, this constraint confines the function $h(T)$ to a particular form, i.e. $h(T) = \sqrt{-T}+\text{constant}$. This theory gets specific values for the two new parameters, i.e. $n = -1/2 = -s$, and contains six classes of acceptable cosmological solutions and three unacceptable ones with the following remarks, particularly in comparison with the $f(R)$ gravity studied in Ref. [76].

- In all of the solutions, the comparison of the value of the slope of the $m(r)$ curve to -1 is of great importance. This comparison determines the acceptability of the solutions from the cosmological point of view, i.e., there should exist a succession of a saddle radiation era, a saddle matter era and finally a stable accelerated expansion era.
- For all of the fixed points, one of the three conditions (3.18) must be satisfied.
- There is a matter era solution, i.e., P_3, that is always a saddle point which exists for $m \to 0^+$ with both $m'(r) < -1$ and $m'(r) > -1$. In the $f(R)$ gravity, this fixed point is not allowed for $m'(r) < -1$.
- There is an important fixed point, i.e. P_1, with the property $\Omega^{(m)} = 0$ which acts as a stable accelerated expansion point, in addition to the one that already exists in the $f(R)$ gravity. This fixed point is the final attractor in most models of the minimal coupling theory. However, the relevant conditions for this point are

$$m'(r) < -1 \qquad \text{and} \qquad 0 < m < 1/2.$$

- There is a saddle point that indicates a "false" matter era whose scale factor does not behave like the one of matter era (actually, its scale factor behaves as $t^{1/2}$ instead of $t^{2/3}$). This point, which also appears in the $f(R)$ gravity, can exist as the only matter point for some models.
- There is a stable de Sitter point that is the final attractor of the theory. This point appears in the $f(R)$ gravity too, and exists provided that

$$0 < m < 1 \quad \text{at} \quad r = -2.$$

The acceptable cosmological solutions must be a transition from a saddle radiation era to a saddle matter era and finally be able to be connected with an accelerated point as the final attractor, provided that the matter domination should take long enough to form cosmic structures. In principle, in this theory, we have two matter points (one as "standard" and the other as "non–standard" points), two accelerated points and a de Sitter solution. Based on the existence of cosmological solutions, we classify the acceptable solutions into six classes. Two of them have the fixed point P_1 as the final attractor, two have transitions to some regions of P_2, and for the last two, P_8 acts as a de Sitter solution. All these classes of solutions are new ones with respect to $f(R,T)$ gravity, except when the corresponding models have P_8 as a final attractor. However, in $f(R,T)$ gravity, P_8 can be reached after passing by P_1 for some periods. We briefly compare the properties of solutions in terms of acceptable transitions for several specific models in both $f(R,T)$ and the $f(R)$ gravities in Table 3. Numerically, we show that theories with $g(R) = aR^{-\beta}$, $g(R) = R^p \exp(qR)$, $g(R) = R + \alpha R^{-n}$, $g(R) = R^p[\log(\alpha R)]^q$ and $g(R) = R^p \exp(q/R)$ have proper sequences of the radiation–matter–acceleration eras for some values of their space parameters, which indicate that these theories

deserve further investigation. We show that for the corresponding models, in which the cosmological trajectories advance to P_8, the trajectories pass by P_1 before approaching to P_8. Also, we have numerically checked that it is always possible to control the duration in which the trajectories stay around P_1, and the duration of the matter dominated era (the width of matter density parameter in the related diagrams).

In $f(R,T)$ gravity with the minimal coupling, our investigated models can present a standard cosmological history including transient periods of radiation and matter domination followed by a period of accelerated expansion domination, which can also give the presently observed [87] contribution of the density parameters $\Omega_0^{(m)} \simeq 0.3$ and $\Omega_0^{(\mathrm{DE})} \simeq 0.7$. Some of the models can explain the accelerated expansion, via a dark energy with an effective equation of state parameter of about -1. Though for some of the other models, the trajectories are trapped in the point $P_1$and hence, this effective parameter approaches to the value $-1/2$, which contradicts the recent Planck results [87]. Also, our models numerically suggest a power–law behavior of the scale factors (near $z \simeq 0$) of the form $a(t) \propto t^n$ for $1.025 < n < 1.038$, which gives an accelerated epoch and leads to a Hubble parameter of the form $H(z) \propto (1+z)^{1/n}$. These results have been obtained numerically; however, a non–numeric considerations can be performed to reconstruct these models with constant parameters that are consistent with the present values of H_0 and $\Omega_0^{(m)}$. Beyond these preliminary considerations, one can also further constraint the models using the type Ia supernovae measurements, the distance to the baryonic acoustic oscillations and/or the position of the first peak in the spectrum of anisotropies of CMBR observation. Indeed, one can theoretically obtain the Hubble parameter $H(z)$ for each model (which in addition to H_0 and $\Omega_0^{(m)}$, it may be a function of the other constant parameters of the model) then, performs the related calculations (e.g., the distance modulus of a supernova at redshift z) using $H(z)$ and hence, compares statistically the results with the available data (e.g., the observed distance modulus of a supernova) to find out the best values of the parameters of the model. Also, by a further step, one can consider the model at the level of perturbation. That is, by obtaining the effective gravitational constant (which, in general, depends on the constant parameters of the model), one can track the structure formation around the matter era and thus, constrain the parameters of the model (e.g., the scalar perturbations have been considered for some models in Ref. [71]). In a further study of $f(R,T)$ gravity, and in an independent work, it would be our task to present the observational constraints for our models.

The pure non–minimal theory has a few problems both in fundamental and cosmological aspects. First of all, a Lagrangian with the property $h(T) = 0$ at $T = 0$ does not lead to the vacuum solution, and actually one gets a null Lagrangian. In addition, there is another problem in the cosmological regime, namely, there is lack of a matter point. That is, all the fixed points have $\Omega^{(m)} = 0$; see Table 4 for more details.

In the non–minimal theory, the corresponding fixed points consist of the following.

(i): The same matter point as the minimal theory, but with different eigenvalues. This point exists provided that $m \to 0^+$ and $m'(r) > -1$, which is the same as in the $f(R)$ gravity.

(ii): Three fixed points as stable accelerated expansion solutions which are

$$m'(r) < -1, \qquad 0.347 \lesssim m < 1/2, \qquad -1/3 < w^{(\mathrm{eff})} < -0.260,$$
$$m'(r) < -1, \qquad 0.486 \lesssim m < 0.60, \qquad -1 < w^{(\mathrm{eff})} \lesssim -0.75,$$

in the non–phantom domain, and

$$m'(r) > -1, \qquad m > 0.60, \qquad w^{(\mathrm{eff})} < -1,$$

in the phantom domain.

(iii): A stable de Sitter point which exists provided that $0 < m < 1/2$.

Further considerations of the possible transitions and studies of various models of this theory will be reported elsewhere.

ACKNOWLEDGMENTS

We thank the Research Office of Shahid Beheshti University G.C. for financial support.

[1] Farhoudi, M., *Non–linear Lagrangian Theories of Gravitation*, (Ph.D. Thesis, Queen Mary & Westfield College, University of London, 1995).

[2] Capozziello, S. & De Laurentis, M. "Extended theories of gravity", *Phys. Rep.* **509** (2011), 167.
[3] Overduin, J.M. & Wesson, P.S. "Kaluza–Klein gravity", *Phys. Rep.* **283** (1997), 303.
[4] Maartens, R. "Brane–World gravity", *Living Rev. Rel.* **7** (2004), 7.
[5] Faraoni, V., *Cosmology in Scalar–Tensor Gravity*, (Kluwer Academic Publishers, London, 2004).
[6] Farhoudi, M. "On higher order gravities, their analogy to GR, and dimensional dependent version of Duff's trace anomaly relation", *Gen. Rel. Grav.* **38** (2006), 1261.
[7] Nojiri, S. & Odintsov, S.D. "Introduction to modified gravity and gravitational alternative for dark energy", *Int. J. Geom. Meth. Mod. Phys.* **04** (2007), 115.
[8] Sotiriou, T.P. *Modified Actions for Gravity: Theory and Phenomenology*, (Ph.D. Thesis, International School for Advanced Studies, Trieste, 2007).
[9] De Felice, A. & Tsujikawa, S. "$f(R)$ theories", *Living Rev. Rel.* **13** (2010), 3.
[10] Sotiriou, T.P. & Faraoni, V. "$f(R)$ theories of gravity", *Rev. Mod. Phys.* **82** (2010), 451.
[11] Nojiri, S. & Odintsov, S.D. "Unified cosmic history in modified gravity: from $F(R)$ theory to Lorentz non–invariant models", *Phys. Rep.* **505** (2011), 59.
[12] Clifton, T., Ferreira, P.G., Padilla, A. & Skordis, C. "Modified gravity and cosmology", *Phys. Rep.* **513** (2012), 1.
[13] Bertonea, G., Hooperb, D. & Silk, J. "Particle dark matter: evidence, candidates and constraints", *Phys. Rep.* **405** (2005), 279.
[14] Silk, J. "Dark matter and galaxy formation", *Ann. Phys. (Berlin)* **15** (2006), 75.
[15] Feng, J.L. "Dark matter candidates from particle physics and methods of detection", *Annu. Rev. Astron. Astrophys.* **48** (2010), 495.
[16] Frenk, C.S. & White, S.D.M. "Dark matter and cosmic structure", *Ann. Phys. (Berlin)* **524** (2012), 507.
[17] Bergström, L. "Dark matter evidence, particle physics candidates and detection methods", *Ann. Phys. (Berlin)* **524** (2012), 479.
[18] Peebles, P.J.E. "The cosmological constant and dark energy", *Rev. Mod. Phys.* **75** (2003), 559.
[19] Polarski, D. "Dark energy: current issues", *Ann. Phys. (Berlin)* **15** (2006), 342.
[20] Copeland, E.J., Sami, M. & Tsujikawa, S. "Dynamics of dark energy", *Int. J. Mod. Phys. D* **15** (2006), 1753.
[21] Durrer, R. & Maartens, R. "Dark energy and dark gravity: theory overview", *Gen. Rel. Grav.* **40** (2008), 301.
[22] Bamba. K, Capozziello, S., Nojiri, S. & Odintsov, S.D. "Dark energy cosmology: the equivalent description via different theoretical models and cosmography tests", *Astrophys. Space Sci.* **342** (2012), 155.
[23] Persic, M., Salucci, P. & Stel, F. "The universal rotation curve of spiral galaxies–I. The dark matter connection", *Mon. Not. R. Astron. Soc.* **281** (1996), 27.
[24] Catinella, B., Giovanelli, R. & Haynes, M.P. "Template rotation curves for disk galaxies", *Astrophys. J.* **640** (2006), 751.
[25] Weinberg, S., *Cosmology*, (Oxford University Press, New York, 2008).
[26] Guth, A.H. "Inflationary universe: A possible solution to the horizon and flatness problems", *Phys. Rev. D* **23** (1981), 347.
[27] Linde, A.D. "A new inflationary universe scenario: A possible solution of the horizon, flatness, homogeneity, isotropy and primordial monopole problems", *Phys. Lett. B* **108** (1982), 389.
[28] Linde, A.D. "Chaotic inflation", *Phys. Lett. B* **129** (1983), 177.
[29] Linde, A.D. "The inflationary universe", *Rep. Prog. Phys.* **47** (1984), 925.
[30] Brandenberger, R.H. "A status review of inflationary cosmology", *hep-ph/0101119*.
[31] Riess, A.G., *et al.* "Observational evidence from supernovae from an accelerating universe and a cosmological constant", *Astron. J.* **116** (1998), 1009.
[32] Perlmutter, S., *et al.* (The Supernova Cosmology Project), "Measurements of Ω and Λ from 42 high–redshift supernovae", *Astrophys. J.* **517** (1999), 565.
[33] Riess, A.G., *et al.* "BV RI curves for 22 type Ia supernovae", *Astron. J.* **117** (1999), 707.
[34] Tonry, J.L., *et al.* "Cosmological results from high–z supernovae", *Astrophys. J.* **594** (2003), 1.
[35] Knop, R.A., *et al.* (The Supernova Cosmology Project), "New constraints on $\Omega^{(m)}$, Ω_Λ, and w from an independent set of 11 high–redshift supernovae observed with the *Hubble Space Telescope* ", *Astrophys. J.* **598** (2003), 102.
[36] Tegmark, M., *et al.* (SDSS Collaboration), "Cosmological parameters from SDSS and WMAP", *Phys. Rev. D*, **69** (2004), 103501.
[37] Tegmark, M., *et al.* (SDSS Collaboration), "Cosmological parameters from luminous red galaxies", *Phys. Rev. D*, **74** (2006), 123507.
[38] Eisenstein, D.J., *et al.* (SDSS Collaboration), "Detection of the baryon acoustic peak in the large–scale correlation function of SDSS luminous red galaxies", *Astrophys. J.* **633** (2005), 560.
[39] Blake, C., *et al.* "Universal fitting formulae for baryon oscillation surveys", *Mon. Not. R. Astron. Soc.* **365** (2006), 255.
[40] Percival, W.J., *et al.* "Measuring the baryon acoustic oscillation scale using the Sloan Digital Sky Survey and 2dF galaxy redshift survey", *Mon. Not. R. Astron. Soc.* **381** (2007), 1053.
[41] Spergel, D.N., *et al.* (WMAP Collaboration), "First–year Wilkinson Microwave Anisotropy Probe (WMAP) observations: determination of cosmological parameters", *Astrophys. J. Suppl.* **148** (2003), 175.
[42] Spergel, D.N., *et al.* (WMAP Collaboration), "Wilkinson Microwave Anisotropy Probe (WMAP) three years results: implications for cosmology", *Astrophys. J. Suppl.* **170** (2007), 377.
[43] Komastu, E., *et al.* (WMAP Collaboration), "Five–year Wilkinson Microwave Anisotropy Probe (WMAP) observations: cosmological interpretation", *Astrophys. J. Suppl.* **180** (2009), 330.

[44] Jain, B. & Taylor, A. "Cross–correlation tomography: measuring dark energy evolution with weak lensing", *Phys. Rev. Lett.* **91** (2003), 141302.
[45] Damour, T. "General relativity and experiment: a brief review", *Class. Quantum Grav.* **9** (1992), S55.
[46] Will, C.M., *Theory and Experiment in Gravitational Physics*, (Cambridge University Press, New York, Revised ed. 1993).
[47] Turyshev, S.G. "Experimental tests of general relativity: recent progress and future directions", *Phys.-Usp.* **52** (2009), 1.
[48] Iorio, L., *et al.* "Phenomenology of the Lense–Thirring effect in the solar system", *Astrophys. Space Sci.* **331** (2011), 351.
[49] Birrell, N.D., & Davies P.C.W., *Quantum Fields in Curved Space*, (Cambridge University Press, New York, 1982).
[50] Buchbinder, I.L., Odintsov, S.D. & Shapiro, I.L., *Effective Action in Quantum Gravity*, (Institute of Physics Publishing, Bristol, 1992).
[51] Utiyama, R. & Dewitt, B.S. "Renormalization of a classical gravitational field interacting with quantized matter fields", *J. Math. Phys.* **3** (1962), 608.
[52] Pechlaner, E. & Sexl, R. "On quadratic Lagrangians in general relativity", *Commun. Math. Phys.* **2** (1966), 165.
[53] Ostriker, J.P. & Steinhardt, P.J. "Cosmic concordance", *astro-ph/9505066*.
[54] Padmanabhan, H. & Padmanabhan, T. "CosMIn: The solution to the cosmological constant problem", *Int. J. Mod. Phys. D* **22** (2013), 1342001.
[55] Bernard, D. & LeClair, A. "Scrutinizing the cosmological constant problem and a possible resolution", *Phys. Rev. D* **87** (2013), 063010.
[56] Nobbenhuis, S. "The cosmological constant problem, an inspiration for new physics", *gr-qc/0609011*.
[57] Chiba, T., Okabe, T. & Yamaguchi, M. "Kinetically driven quintessence", *Phys. Rev. D* **62** (2000), 023511.
[58] Armendariz-Picon, C., Mukhanov, V. & Steinhardt, P.J. "Dynamical solution to the problem of a small cosmological constant and late–time cosmic acceleration", *Phys. Rev. Lett.* **85** (2000), 4438.
[59] Chiba, T. "$1/R$ gravity and scalar–tensor gravity", *Phys. Lett. B* **575** (2003), 1.
[60] Dolgova, A.D. & Kawasaki, M. "Can modified gravity explain accelerated cosmic expansion?", *Phys. Lett. B* **573** (2003), 1.
[61] Erickcek, A.L., Smith, T.L. & Kamionkowski, M. "Solar system tests do rule out $1/R$ gravity", *Phys. Rev. D* **74** (2006), 121501.
[62] Li, B. & Barrow, J.D. "Cosmology of $f(R)$ gravity in the metric variational approach", *Phys. Rev. D* **75** (2007), 084010.
[63] Harko, T., Lobo, F.S.N., Nojiri, S. & Odintsov, S.D. "f(R,T) gravity", *Phys. Rev. D* **84** (2011), 024020.
[64] Houndjo, M.J.S. "Reconstruction of $f(R,T)$ gravity describing matter dominated and accelerated phases", *Int. J. Mod. Phys. D* **21** (2012), 1250003.
[65] Alvarenga, F.G., Houndjo, M.J.S., Monwanou, A.V. & Chabi Orou, J.B. "Testing some $f(R,T)$ gravity models from energy conditions", *J. Mod. Phys.* **04** (2013), 130.
[66] Houndjo, M.J.S. "Thermodynamics in little rip cosmology in the framework of a type of $f(R,T)$ gravity", *gr-qc/1207.1646*.
[67] Sharif, M. & Zubair, M. "Thermodynamics in $f(R,T)$ theory of gravity", *J. Cosmol. Astropart. Phys.* **03** (2012), 028.
[68] Jamil, M., Momeni, D. & Ratbay, M. "Violation of the first law of thermodynamics in $f(R,T)$ gravity", *Chin. Phys. Lett.* **29** (2012), 109801.
[69] Farasat, S.M., Jhangeer, A. & Bhatti, A.A. "Exact solutions of Bianchi types I and V models in $f(R,T)$ gravity", *gr-qc/1207.0708*.
[70] Jamil, M., Momeni, D., Muhammad, R. & Ratbay, M. "Reconstruction of some cosmological models in $f(R,T)$ gravity", *Eur. Phys. J. C* **72** (2012), 1999.
[71] Alvarenga, F.G., de la Cruz-Dombriz, A., Houndjo, M.J.S., Rodrigues, M.E. & Sáez-Gómez, D. "Dynamics of scalar perturbations in $f(R,T)$ gravity", *Phys. Rev. D* **87** (2013), 103526.
[72] Farhoudi, M. "Classical trace anomaly", *Int. J. Mod. Phys. D* **14** (2005), 1233.
[73] Odintsov, S.D., & Sáez-Gómez, D. "$f(R,T,R_{\mu\nu}T^{\mu\nu})$ gravity phenomenology and ΛCDM universe", *gr-qc/1304.5411*.
[74] Haghani, Z., Harko, T., Lobo, F.S.N., Sepangi, H.R. & Shahidi, S. "Further matters in space–time geometry: $f(R,T,R_{\mu\nu}T^{\mu\nu})$ gravity", *Phys. Rev. D* **88** (2013), 044023.
[75] Iorio, L. & Saridakis, E.N. "Solar system constraints on $f(T)$ gravity", *Mon. Not. R. Astron. Soc.* **427** (2012), 1555.
[76] Amendola, L., Gannouji, R., Polarski, D. & Tsujikawa, S. "Conditions for the cosmological viability of $f(R)$ dark energy models", *Phys. Rev. D* **75** (2007), 083504.
[77] Lovelock, D. & Rund, H., *Tensors, Differential Forms and Variational Principles*, (Wiley, New York, 1975).
[78] d'Inverno, R. "Introducing Einstein's Relativity", (Clarendon Press, Oxford, 1992).
[79] Wainwright, J. & Ellis, G.F.R. (Eds.), *Dynamical Systems in Cosmology*, (Cambridge University Press, New York, 1997).
[80] Farajollahi, H. & Salehi, A. "Attractors, statefinders and observational measurement for chameleonic Brans–Dicke cosmology", *J. Cosmol. Astropart. Phys.* **11** (2010), 006.
[81] Farajollahi, H. & Salehi, A. "Stability analysis and observational measurement in chameleonic generalised Brans–Dicke cosmology", *J. Cosmol. Astropart. Phys.* **07** (2011), 036.
[82] Haghani, Z., Sepangi, H.R. & Shahidi, S. "Cosmological dynamics of brane $f(R)$ gravity", *J. Cosmol. Astropart. Phys.* **02** (2012), 031.
[83] Amendola, L., Polarski, D. & Tsujikawa, S. "Are $f(R)$ dark energy models cosmologically viable?", *Phys. Rev. Lett.* **98** (2007), 131302.
[84] Amendola, L., Polarski, D. & Tsujikawa, S. "Power–laws $f(R)$ theories are cosmologically unacceptable", *Int. J. Mod. Phys. D* **16** (2007), 1555.
[85] Abdelwahab, M., Carloni, S. & Dunsby, P.K.S. "Cosmological dynamics of 'exponential gravity' ", *Class. Quantum Grav.* **25**, (2008), 135002.

[86] Amendola, L. "Coupled quintessence", *Phys. Rev. D* **62** (2000), 043511.
[87] Ade, P.A.R., *et al.* "Planck 2013 results. XVI. cosmological parameters", *astro-ph/1303.5076*.